International Journal of Sustainable Energy

Characteristic study, its identification and self-tuned approach to control hydro-power plants

A. S. Raghuvanshi, Nand Kishor, Jesus Fraile-Ardanuy & S. P. Singh

1. Introduction

Many studies have been reported for better performance, safe and reliable operation of hydro-power plant (HPP). The power plant though designed to give optimum performance at rated conditions, usually operates on off-design plant parameters due to variation in the load demand. Conventionally, the controller design is normally based on a fixed parameter model of the plant derived by linearisation methods. This seeks importance in the investigation of transient behaviour of the plant. The plant parameters are a function of the operating points. Therefore, as the operating condition changes, the HPP performance with controllers designed for a specific operating point is most likely to be unsatisfactory. Consequently, the nonlinear characteristic makes it difficult to ensure stability for all operating points with conventional controllers. Thus, nonlinear models are required, which is capable to take into account all the dynamics of the system. A nonlinear model should include the effect of water compressibility, i.e. inclusion of transmission-line-like reflections which occur in the elastic-walled pipe carrying compressible fluid. The elastic effect is represented by a delay e^{-2sT_e} in the hydraulic structure. In this term, T_e is the elastic time constant of penstock.

The modelling is more important in a system with long penstock. An interesting area for control theory and application is in the study of a penstock-turbine model with elastic water column effect.

Of the numerous literatures (Hagihara et al. 1979; Murthy and Hariharan 1983; Sanathanan 1987; Lansberry, Wozniak, and Goldberg 1992) on the governor design or stability studies of the hydro-plant, the simple first-order (FO) model neglecting the water column elasticity effect in penstock has been used. Hagihara et al. (1979) established the stability boundaries of the turbine-generator unit having a proportional-integral-derivative (PID) governor using the root locus method. The gate dynamics have been neglected in the study. Murthy and Hariharan (1983) too have considered the same model in the study. The irrational transfer function (TF) model that represents water compressibility and penstock-wall elasticity is reduced to the second-order (SO) form in Sanathanan (1987). Lansberry, Wozniak, and Goldberg (1992) have used the genetic algorithm (GA) optimisation approach for optimal governor tuning. This paper investigates the GA as one possible means of adaptively optimising the gains of proportional-plus-integral governors. This tuning methodology is adaptive towards changing plant parameters-conduit time constant T_{wp} and load self-regulation.

An identification approach to develop the TF model of a 115 MVA generation unit at the Mt. Elbert pumped storage power plant is described in Trudnowski and Agee (1995). The authors (Trudnowski 1992) have used identification tool (SYSFIT) algorithms to determine the fifth-order TF model for the said plant having a water time constant (WTC) of 4 s, which is classified into long penstocks. The approach uses experimental data of a generation unit, obtained by injecting signals into the wicket gate portion. An SO approximation of irrational term e^{-2sT_e} in the TF for the Dinorwing pumped storage HPP is determined in Mansoor et al. (2000). Similarly, Eker (2004) suggests the validity of the FO and lumped parameter from TF up to 1.0 and 10 rad/s, respectively. The investigation of these TF models for the transient study is not described.

The approximation of a high-order system by a low-order seeks importance as it involves less computation time of the transient response (Sanathanan 1987) and is thus suitable in the controller design and control system analysis. The cost and complexity of the controller increase with the system order. Padé (Lam 1993) and H-infinity (Al.-Amer and Al.-Sunni 2000) methods have been utilised in the development of rational low-order TF and their response simulated to find its suitability in system studies (Kishor, Singh, and Raghuvanshi 2006). The authors discuss the static and dynamic simulations behaviour for FO, SO, third-order (TO) and fourth-order (FR) TF models of a HPP. The nonlinear dynamic effect is illustrated with multi-step input as a gate position variation. The authors (Nicolet et al. 2007) present the TF model of a 4×250 MW Francis turbine determined through a time-domain simulation, using the white noise excitation signal as the input variable and the rotational speed as the output variable. The nonlinear characteristics of the hydraulic turbine and the inelastic water hammer effect are considered to calculate and simulate hydraulic transients in Fang et al. (2008). The influence of PID controller gains, WTC and surge tank dimension was analysed to study the dynamic stability of the hydro-turbine regulating system. However, the authors have not mentioned whether optimal PID gains were determined or not. Recently, nonlinear differential equations of hydro-turbine under elastic water column are modelled and its reduced order reflects dynamic characteristic (Zeng et al. 2011).

The well-known dimensionless parameters WR^2 and L_p/Γ_p ratio in association with reference speed, flow, etc. define mechanical time constant (MTC), T_m and WTC, T_{wp}. Reduced values of T_{wp} and increased value of T_m lead to a small speed deviation, but are not economically desirable. Extensive studies have been conducted in the modelling of non-elastic effects (Hagihara et al. 1979; Murthy and Hariharan 1983; Sanathanan 1987) and governor parameters tuning (Lansberry, Wozniak, and Goldberg 1992; Eker 2004) for assumed values of T_{wp} and T_m. The response time of the hydro-plant is predominantly determined by the WTC, and the response time varies in the range from 20 to 120 s depending upon the length of the penstock.

Additionally, in a stand-alone/small-size power system during the black-start, the values of WTC, T_{wp} and damping coefficient D_{m} greatly affects the stability of the governor operation. However, most of the studies focus on start-up and shut-down behaviour of the power plant. Few works provide the operational plan during load ramping or oscillation, etc. Therefore, a reasonable estimation of the operational characteristic of the whole plant during any transient operation (shut-down and start-up, load ramping, load oscillation, equipment failure, etc.) is essential for a safe operation and reliable control. In fact, the time involved in gate-closure is also important in keeping the minimum hydraulic transients caused due to the water hammer phenomenon.

This paper aims to carry out the analytical study of the HPP dynamics when elastic effects in the penstock have been approximated to lower order models, under different nature of input signals, WTC and MTC. Identification of discrete-time (DT) domain models and their characteristic representation is discussed next. Also, the use of self-tuning approach to minimise the speed deviations under various conditions is presented at the end.

2. Hydro-power plant's mathematical representation

For a small variation around an operating point, the linearised equation of the turbine can be given as (Sanathanan 1987):

$$\Delta q_t = a_{11}\Delta h_{\mathrm{t}} + a_{12}\Delta g_{\mathrm{open}} + a_{13}\Delta\omega_{\mathrm{r}}, \tag{1}$$

$$\Delta p_{\mathrm{develop}} = a_{21}\Delta h_{\mathrm{t}} + a_{22}\Delta g_{\mathrm{open}} + a_{23}\Delta\omega_{\mathrm{r}}. \tag{2}$$

The turbine constants a_{ij} are the partial derivatives of flow and torque with respect to head, gate position and turbine speed. The a_{ij} coefficients depend on turbine loading and may be evaluated from the turbine characteristics at any operating point. Their values remain constant for the variation near the turbine-rated operating point $(q_{\mathrm{o}}, p_{\mathrm{o}})$. These values have to be measured accurately or determined from turbine model tests.

The symbol Δ denotes the deviation from the steady-state operating point. The penstock TF relating to the incremental head and flow in terms of complex frequency s can be written as (Sanathanan 1987):

$$\frac{\Delta H_{\mathrm{devia,p}}(s)}{\Delta Q_{\mathrm{p}}(s)} = -Z_{\mathrm{p}}\tanh(sT_{\mathrm{e}} + F_{\mathrm{p}}). \tag{3}$$

Equation (3) depends only on the length of the penstock and is independent of the turbine characteristics.

In Equation (3), Z_{p} is the normalised hydraulic surge impedance which is given as follows:

$$Z_{\mathrm{p}} = \frac{T_{\mathrm{wp}}}{T_{\mathrm{e}}}, \tag{4a}$$

where T_{wp} is the water starting time (i.e. WTC or water disturbance) and T_{e} is the wave travel time (i.e. elastic time constant), which are defined as

$$T_{\mathrm{wp}} = \frac{L_{\mathrm{p}}Q_0}{H_0\Gamma_{\mathrm{p}}g_a}, \tag{4b}$$

$$T_{\mathrm{e}} = \frac{L_{\mathrm{p}}}{v_{\mathrm{p}}}. \tag{4c}$$

WTC is a function of water flow, turbine head and the length of the penstock. An irrational TF of the penstock-turbine with elastic water column effect, neglecting hydraulic friction loss derived

from Equations (1) and (2) relates the ratio of incremental torque to changes in the gate position and is given as (Sanathanan 1987):

$$\frac{\Delta P_{\text{develop}}(s)}{\Delta G_{\text{open}}(s)} = \frac{a_{23} + (a_{11}a_{23} - a_{21}a_{13})Z_{\text{p}} \tanh(sT_{\text{e}})}{1 + a_{11}Z_{\text{p}} \tanh(sT_{\text{e}})}. \tag{5}$$

It is difficult to use Equation (5) in its present form for system stability studies. It is often helpful to have a finite-dimensional approximation of the TF. The delay term $\text{e}^{-2sT_{\text{e}}}$ in Equation (5) can be converged to a low order, and the derivation of the rationalised approximate TF of FO, SO, TO and FR using Padé and H-infinity techniques is given in Kishor, Singh, and Raghuvanshi (2006). These TFs are shown to represent similar characteristics as with rationalised TF with $n_{\text{w}} = 1$ (i.e. the fundamental component of the water column). It should be noted that the hydro-turbine governing system and WTC T_{wp} are important parameters of the plant. It has a very strong influence on the system stability and dynamical performance. It is T_{wp} that causes the location of a right-hand zero on the s-plane, thus making the system become a non-minimum phase. The WTC depends on the load and MTC T_{m} is related to the angular speed of the turbine-generating set.

3. Characteristic study

The dynamic and static behaviours of the hydro-plant must be determined to examine the nonlinear characteristics. This section describes the turbine power response at different values of WTC, $T_{\text{wp}} = 3, 4, 5$ & 6 s with plant parameters given in the appendix

3.1. *Dynamic variation*

The dynamic nonlinear effects are shown in time- and frequency-domain. The transient characteristic is determined by examining the variation in turbine power with sudden change in the gate position. The unit step response for FO, SO, TO and FR TF models with $T_{\text{wp}} = 3$ s is presented in Figure 1. The well-known non-minimum phase characteristic is illustrated. The initial response to opening of the gate is independent of the model order. The intersection of the zero power line with the delay line (Figure 1(b)) suggests delay in power demand with respect to gate change, which leads to a serious consequence on target power tracking. A close observation reveals that the delay varies in the order of 1.2–1.4 s. The elastic-wave effect as pressure dynamics representation is observed only in the case of TO and FR models. It is further suggested that the characteristic variation for the SO and the TO model lies in-between the FO and the FR ones. Thus, due to space limitation in the paper, the analyses of the results for the FO and the FR TF models are only presented.

The frequency response characteristics for FO and FR TFs are illustrated in Figure 2. One can notice that the frequency responses of the H-infinity and Padé models are very similar even though their parameters are significantly different. The validity of the FO and FR TF models are observed up to 1.0 and 10 rad/s, respectively. The gain and phase margin vary with the flow through the turbine, i.e. WTC. The variations are identical in the low frequency range (0.01–1 rad/s). The variations of the FO H-infinity and Padé TF response are approximately similar with an exception to Padé TF at $T_{\text{wp}} = 6$ s. In this case, it seems that the model behaviour approaches those of higher order ones. However, in case of the FR model, an increase in WTC results in the reduction of the phase margin, and subsequently the loss of stability.

The developed turbine power response as a function of time on the unit step gate position changes with different WTCs value is represented in Figure 3. The initial inverse power change in the case of the FO and the FR model is observed to be of the same value. And the subsequent

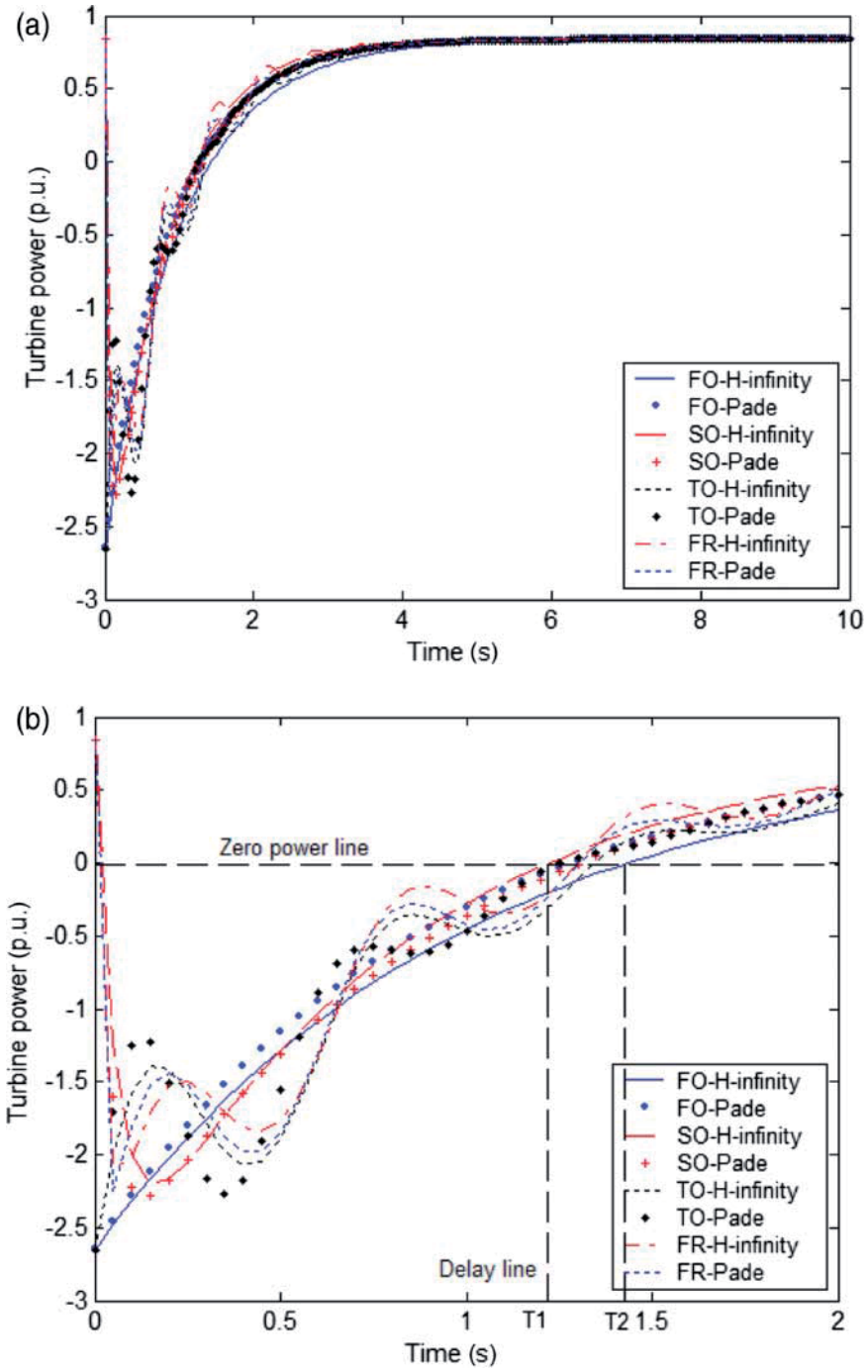

Figure 1. Developed power response on unit step gate position change for different orders of TF models with $T_{wp} = 3$ s. (a) Detailed characteristics and (b) zoomed characteristics.

increase in power depends on the WTC. The delay in response with the higher flow (i.e. WTC) is illustrated. The speed of power demand changes, either increase or decrease determines the initial speed (frequency) response in the closed loop operation. Thus, a higher WTC comparatively

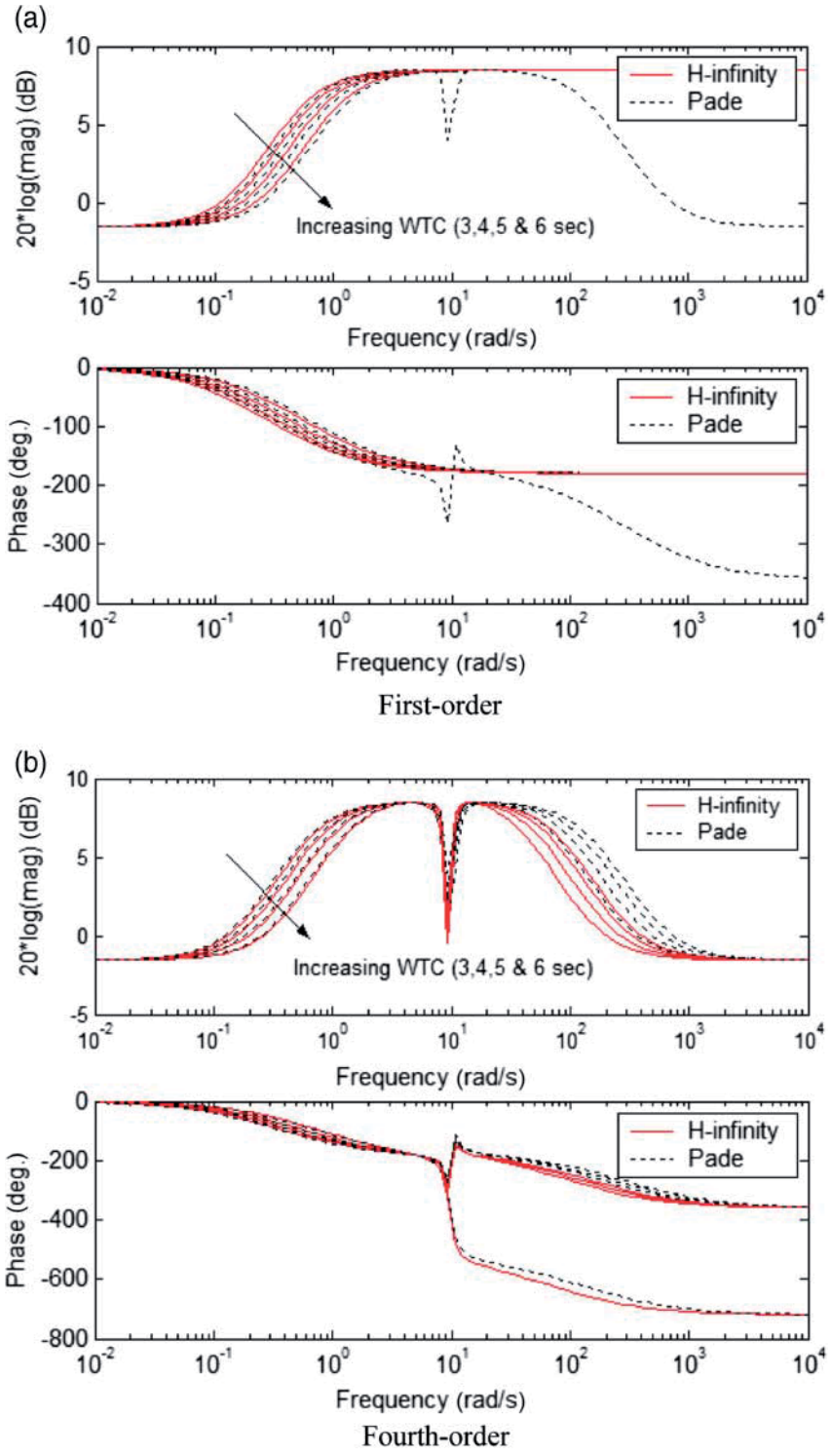

Figure 2. Frequency response of HPP models at different values of WTC. (a) FO and (b) FR.

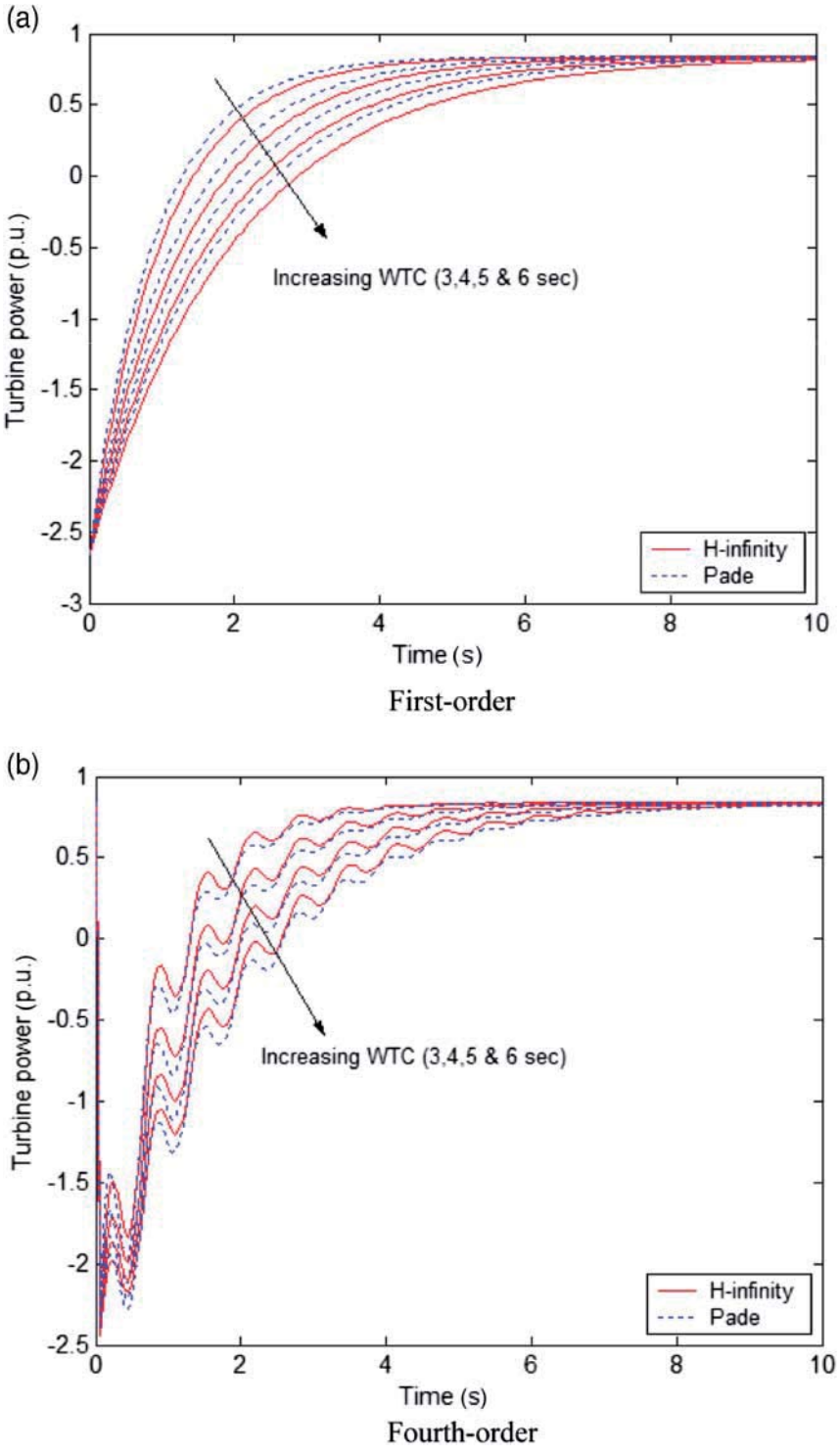

Figure 3. Developed power response on unit step gate position change at different values of WTC. (a) FO and (b) FR.

Table 1. Time-domain step response characteristics of FR TF model.

	Rise time (s)		Undershoot (%)		Settling time (s)		Maximum time (s)	
WTC (s)	H-infinity TF	Padé TF	H-infinity TF	Padé TF	H-infinity TF	Padé TF	H-infinity TF	Padé TF
3	0.0021752	0.0023651	357.8724	372.0916	4.4983	4.6119	4.4983	4.995
4	0.002998	0.0032248	374.9974	385.6767	5.9271	6.3625	5.996	6.9914
5	0.0038024	0.0040711	385.1832	393.4925	7.2968	7.8532	7.985	8.9891
6	0.0045982	0.0049113	391.9768	398.5574	9.1504	9.5918	9.9873	9.9994

requires a greater control effort. The elastic-wave effect as pressure dynamics representation in the FR TF model is also evident. The time-domain step response characteristics of the FR TF models are further illustrated in Table 1.

The response against the sudden changes in the gate position by a small amount (0.2 p.u.) at a regular interval is shown in Figure 4. A definite conclusion cannot be drawn from the time-response as shown in Figure 4(a) and 4(b). Thus, the zoomed variation on rise- and fall-step is obtained and shown in Figure 4(c)–(f). The initial inverse power response with respect to the gate position change is represented and these vary as a function of the WTC. It is evident that with a small magnitude step change (both rise and fall), the dynamic variation for the FR model is almost identical to the FO, i.e. the elastic-wave effect gets suppressed. The difference between the two simulations is negligible. In other words, power dynamics due to pressure oscillations get eliminated on the small step change in gate position. For the comprehensive work considered here, the above study suggests a measure of the maximum rate of change in the turbine power determined by the limit on gate opening/closing rate. However, further study could be investigated to determine the upper limit of the step change up to which the elastic-wave effect is not reflected in the power response.

Next, the simulation study on the ramped gate position change is analysed as shown in Figure 5. Nevertheless, in this case, the characteristic of FO and FR TFs are found to be identical. The zoomed power response given in Figure 5(c) and 5(d) suggests a steady rise with corresponding the ramped gate position change. A close observation further reveals a small (0.035 p.u.) initial positive/negative power response.

With the above discussion, it is understood that the variation in the turbine power response is attributed to the changes in the gate position; its amount and rate of opening/closing. The response of the FR model (with approximate elastic effects) on small magnitude change eliminates the pressure-wave dynamics in turbine power.

3.2. *Steady-state study*

As it is well-known, the developed turbine power is a nonlinear function of the gate position. This relationship holds true for all the turbine designs and is unique to each type. Nevertheless, the general characteristics of the plant models are illustrated in Figure 6(a) for a WTC equal to 3, 4, 5 and 6 s. The variation illustrates that the relationship between the turbine power and gate position will have a slope deviated from the linear one. As observed for low order (i.e. FO) models, the determined steady-state characteristic is independent of the time constant (WTC), i.e. this model suppresses the characteristics at different values of WTC. However, for the FR models and at a higher range of the gate position, the dependency may be found. In other words, the model needs to be remodelled for different loading conditions and thus the nonlinearity between the turbine power and the gate position will be determined by the associated WTC value. This suggests that for small WTC, i.e. load conditions, the first model representation is accurate, but for large disturbances, the higher order model is required to be considered in the analysis. This seeks

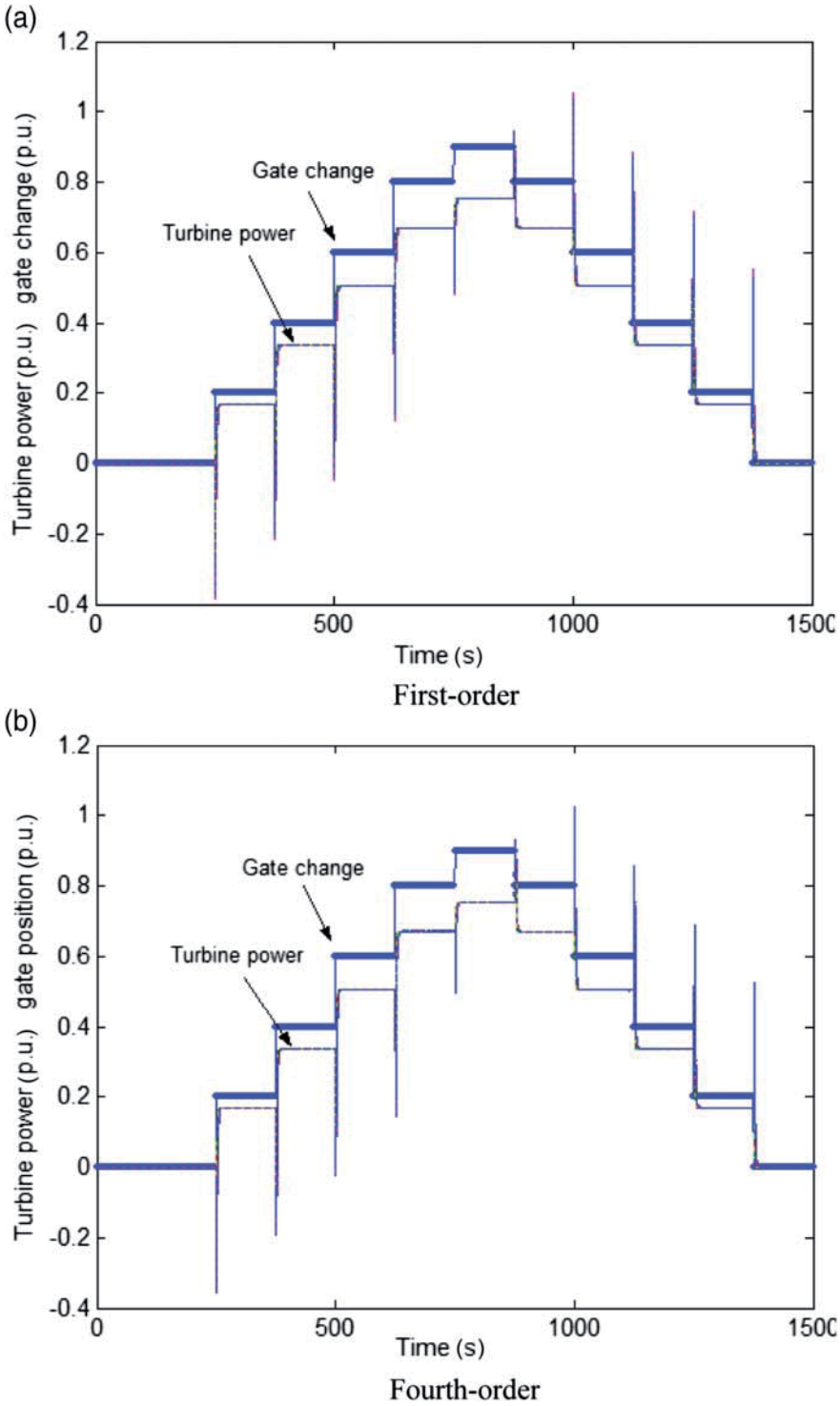

Figure 4. Developed power response on multi-step gate position change at different values of WTC. (a) FO, (b) FR, (c) zoomed on rise-step: FO, (d) zoomed on rise-step: FR, (e) zoomed on fall-step: FO and (f) zoomed on fall-step: FR.

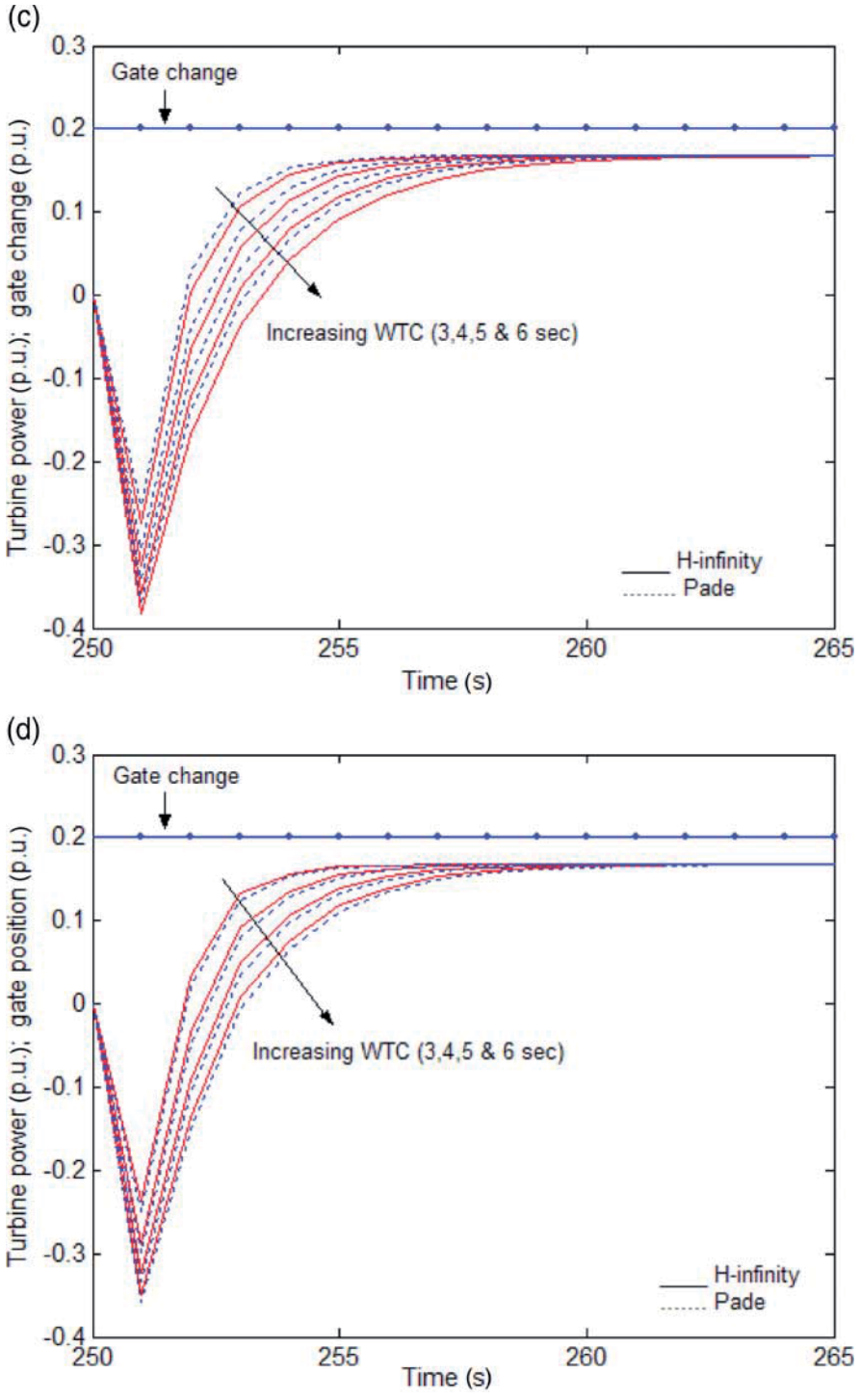

Figure 4. Continued.

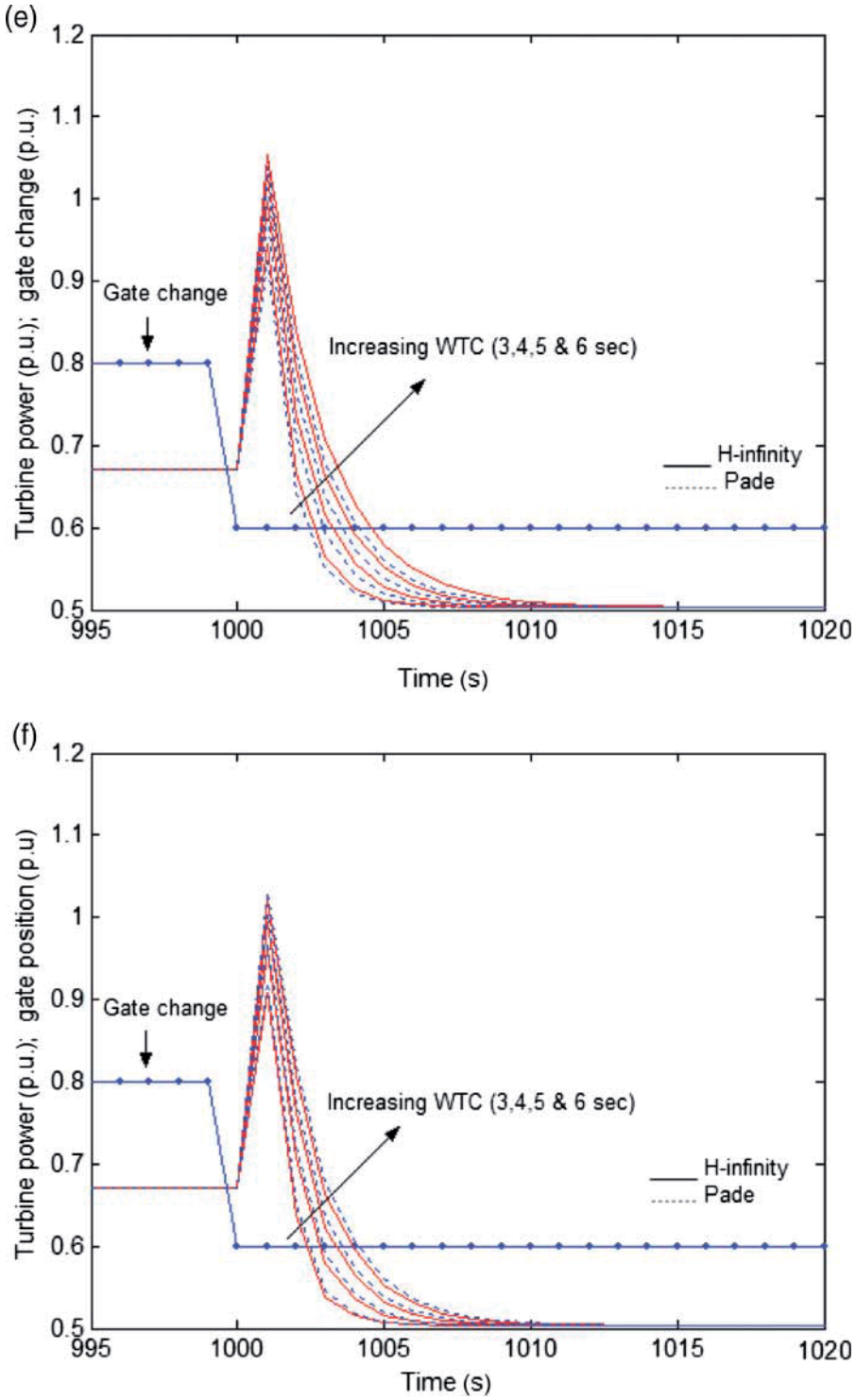

Figure 4. Continued.

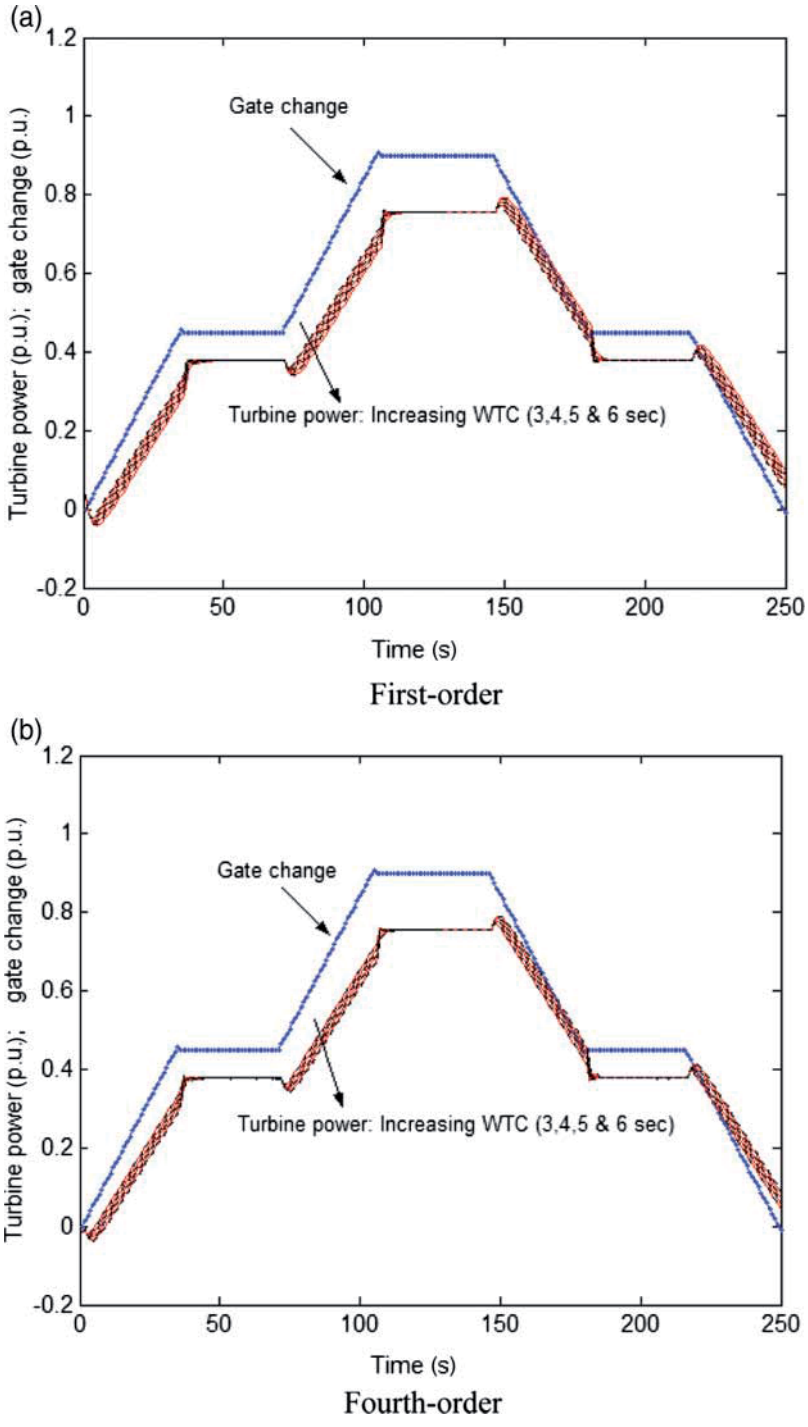

Figure 5. Developed power response on ramped gate position change at different values of WTC. (a) FO, (b) FR, (c) zoomed: FO and (d) zoomed FR.

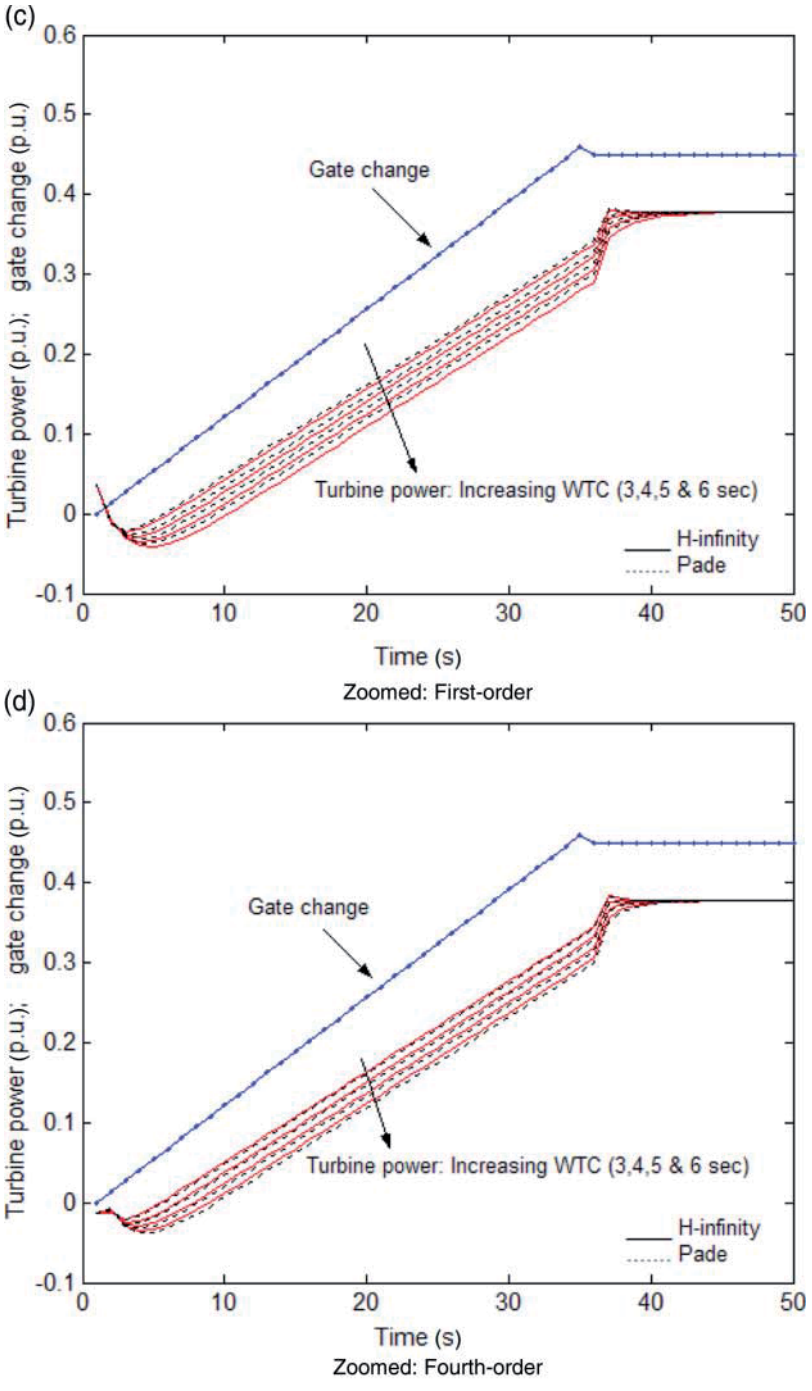

Figure 5. Continued.

major importance in the controller design for a hydro-plant with a long penstock. The developed turbine power will deviate much from the droop-setting value. The variations of turbine power suggest that the power loss percentage is constant irrespective of WTC values and remains the same for both FO and FR models.

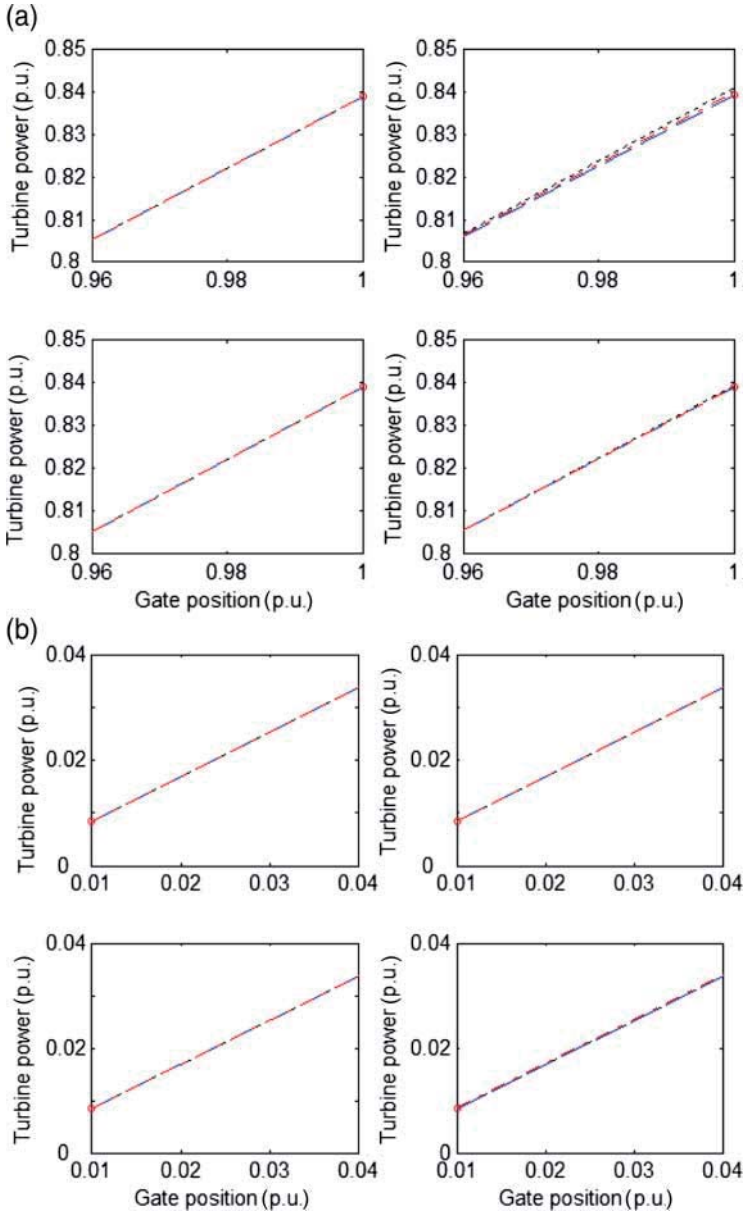

Figure 6. Developed power response as a function of gate position. Upper panel-H-infinity model: FO (11), FR (12); lower panel-Padé model: FO (21), FR (22). (a) Variation on higher range gate position and (b) variation on lower range gate position.

4. Characteristic identification

System identification is an established field in the area of system analysis and control. It deals with the problem to determine simplified mathematical models of dynamical systems based on input–output time-series measurement data (Flores and Pastor 2005). An optimisation technique is applied to search a model from a space of possible models. The conventional least-square (LS) method has been popular for the system identification due to its simplicity in computation

and a high rate of convergence. However, the said approach results in biased or non-consistent estimates of system parameters. A number of methods such as the generalised LS, extended matrix, maximum likelihood or instrumental variable (IV) have been suggested to remove the bias (Söderström and Stoica 1989). The IV-based approaches for the DT model are said to be robust against the properties of the noise (Young 1984). The IV techniques do not require *a priori* knowledge of the noise statistics. State-variable filter (SVF) is one of the deterministic approaches that belong to method IV. The said technique used in refined IV for DT model algorithms (Young 1984; Captain Toolbox 2007) is considered in the study for the identification of turbine power dynamics with regard to gate position.

4.1. *Identification problem formulation*

Consider a linear, single-input, single-output, DT domain sampled data equation form as follows:

$$y_{\mathrm{un},k} + a_1 y_{k-1} + + a_n y_{k-n} \cdots = b_1 u_{k-\delta} + \cdots + b_m u_{k-\delta-m} + \upsilon_k, \tag{6}$$

where $y_{\mathrm{un},k}$ and u_k are, respectively, the turbine-developed power and gate-position at the kth sampling instant, δ denotes any pure, 'advective' time delay, υ_k represents the noise, considered as the zero mean stationary, serially uncorrelated Gaussian white noise, m, n define the model order.

Equation (6) can also be written in the TF form as follows:

$$y(k) = \frac{B(q^{-1})}{A(q^{-1})} u(k) + \upsilon(k), \tag{7}$$

$$y(k) = y_{\mathrm{un}}(k) + \upsilon(k) \tag{8}$$

where q^{-1} is the backward shift operator, i.e. $q^{-1}u(k) = u(k-i)$. The measured output $y(k)$ is assumed to be corrupted by an additive measurement noise $\upsilon(k)$.

The polynomials $A(q^{-1})$, $B(q^{-1})$ are defined as

$$A(q^{-1}) = 1 + a_1 q^{-1} + \cdots + a_n q^{-n}, \tag{9}$$

$$B(q^{-1}) = b_1 q^{-1} + \cdots + a_m q^{-m}. \tag{10}$$

The RIVD algorithm (Flores and Pastor 2005) uses iteratively an auxiliary model whose output can be computed by

$$y_u(k, \hat{\theta}_i) = \frac{\hat{B}_i(q^{-1})}{\hat{A}_i(q^{-1})} u(k) \tag{11}$$

with an SVF given as follows:

$$y_f(k, \hat{\theta}_i) = \frac{1}{\tilde{A}_i(q^{-1})} y(k), \tag{12}$$

where $\hat{\theta}_i$ denotes the estimated parameter vector at the ith iteration. The details of the algorithms can be obtained from Captain Toolbox (2007).

4.2. *Modelling illustration*

To illustrate the capability of the identification method as shown above and given in Captain Toolbox (2007), the H-infinity and Padé TFs of the FO, SO, TO and FR are simulated with

the seventh-order pseudorandom binary signal (PRBS) and the multi-step signal as input (gate-position) to obtain output data (turbine-developed power). In the identify-then-control approach, it is desirable to consider additive perturbations of the nominal TFs or take into account the variable plant structure. To illustrate the effectiveness and performance, the simulated output $y(k)$ is corrupted with the noise content. Monte-Carlo simulations are performed to generate noise for a SNR given as

$$\mathrm{SNR} = 10 \log \frac{W_y}{W_v}, \tag{13}$$

where W_y denotes the average power of the noise-free output variation, while W_v represents the average power of the zero-mean additive noise. The output with the noise content is said to be the estimation of the data set. And models are validated from the data set without the noise content. The statistical measures called the coefficient of determination (CoD) are given as (Söderström and Stoica1989)

$$R_T^2 = 1 - \frac{\hat{\sigma}_\varepsilon^2}{\hat{\sigma}_y^2}, \tag{14}$$

where $\hat{\sigma}_y^2$ and $\hat{\sigma}_\varepsilon^2$ denote the variance of the generated output and the variance of the error between the generated output and simulated model output, respectively.

And Young's Information Criterion (YIC) is given as (Captain Toolbox 2007)

$$\mathrm{YIC} = \log_\mathrm{e}\left[\frac{\hat{\sigma}_\varepsilon^2}{\hat{\sigma}_\varepsilon^2}\right] + \log_\mathrm{e}\frac{1}{p}\sum_{j=1}^{p}\frac{\hat{\sigma}_\varepsilon^2 p_{jj}}{\hat{a}_j^2} \tag{15}$$

is calculated on the validation data set and used to choose between a range of model orders.

In Equation (15), $\hat{a}_j^2$ is the square of the jth estimated parameter, p_{jj} is the jth diagonal element of the refined instrumental variable discrete (RIVD) estimated parameter error covariance matrix $\hat{\mathrm{P}}$ and p is the number of parameters. Solving RIVD (Captain Toolbox 2007), the statistical measure of the model parameterisation is obtained with either CoD or YIC. The value of CoD indicates how well the model output fits into the developed turbine power and must be close to unity. Between the two, YIC is a better choice since R_T^2 tends to overestimate. The greater negative value of YIC ensures a better model fit. The appropriate model structure/order is selected from 10 different models according to the best value of the YIC criterion.

Due to space limitation in the paper, comparison among the output of the models is represented in the form of CoD and YIC values. Table 2 lists the model output performance statistics without the noise content and with the output signal corrupted with 10 and 20 dB SNRs, when excited by multi-step and PRBS input signals. It can be observed that the identified output performances for both H-infinity and Padé TFs are close to each other. The validity of the identified output and thus the estimated parameters for the FO TF when excited by both the type of input signals does not vary significantly in terms of CoD values. For higher order TFs, as expected, the estimation of parameter deteriorates. A close observation indicates further that the excitation signal with a uniform change in magnitude and interval does not affect the identification performance between FO and FR TFs. However, the validity does depend on the random variation of input signals. The statistical value suggests the models to have approximately 99% (100%) and 92% (99%) variance in data without noise content for the FR and the FO when excited by multi-step and PRBS input signals, respectively.

The cross-validation results obtained with the multi-step input signal for the FR H-infinity TF output with 10 and 20 dB SNRs are shown in Figure 7. As suggested from the magnitude of the developed power variation, the identified model dynamics are well represented, close to the simulated output. The output power varies in accordance to step increase (gate-opening)

Table 2. Statistical attributes in modelling the hydro-turbine characteristic.

YIC

	Without noise		With noise content			
			10 dB		20 dB	
	H-infinity	Padé	H-infinity	Padé	H-infinity	Padé
(a) *Multi-step gate-position input signal*						
Order						
First	−103.31	−99.50	−8.63	−8.44	−12.90	−12.83
Fourth	−10.17	−10.06	−8.04	−8.62	−11.31	−11.13
R_T^2-						
First	1.0	1.0	0.908370	0.909397	0.990063	0.990143
Fourth	0.997093	0.997127	0.902350	0.875657	0.982274	0.981092
(b) *PRBS*						
Order						
First	−32.03	−32.08	−10.64	−10.68	−15.20	−15.16
Fourth	−11.48	−11.09	−9.67	−9.39	−11.17	−10.85
R_T^2-						
First	0.999998	0.999998	0.907513	0.910002	0.990079	0.990055
Fourth	0.937936	0.924428	0.854941	0.836688	0.928309	0.915471

and step decrease (gate-closing). The identified output does represent the non-minimum phase characteristic as shown in Figure 7(c).

The above discussion further reveals that an approximately 0.15 p.u. step-change at regular intervals does not lead to the elastic-wave represented in the simulated output and thus in the identified output. And with a large change (unit step), identified output fails to represent the wave dynamics as similar to the simulated output.

Next, the unit step response of the identified DT model and the simulated output is shown in Figure 8. The test results illustrated in Figure 8(a) indicate the perfect modelling match, nevertheless, in case of data with noise content; there is some error in a steady-state region of the curve, as indicated in Figure 8(c). Furthermore, the observations in Figure 8(b) and 8(d) suggest that the dynamics of the FR TF is not represented accurately, since the DT model is identified from the data pertaining to those input excitation signals which eliminates the wave-effects in power characteristics. The error in the parameter estimation caused the model response to have a delay relative to the simulated output.

The technique discussed above is validated in identifying the hydro-turbine characteristic with those discussed in Trudnowski and Agee (1995). The authors have identified the TF model of 115 MVA hydro-turbine unit based on measured data of different gate positions and output powers using SYSFIT algorithms. The identified TF model determined by the SYSFIT at a load of 25, 50 and 75 MW is simulated with the multi-step gate position input signal and shown in Figure 9. As observed, the hydro-turbine output characteristic is similar to those discussed in Figure 7. Further, the frequency and time-domain response comparison of these identified TF models with the FR, H-infinity TF model is illustrated in Figure 10. The occurrence of resonance (R) and anti-resonance (AR) conditions is also indicated in Figure 10(a).

The validation of the suggested study is now presented in the identification of the DT model with those obtained by the SYSFIT technique. The unit step response of these models is shown in Figure 11. For each load condition, the hydro-turbine power characteristic is satisfactorily demonstrated. In addition, the quantitative analysis to validate the efficiency of characteristic identification is presented in Table 3.

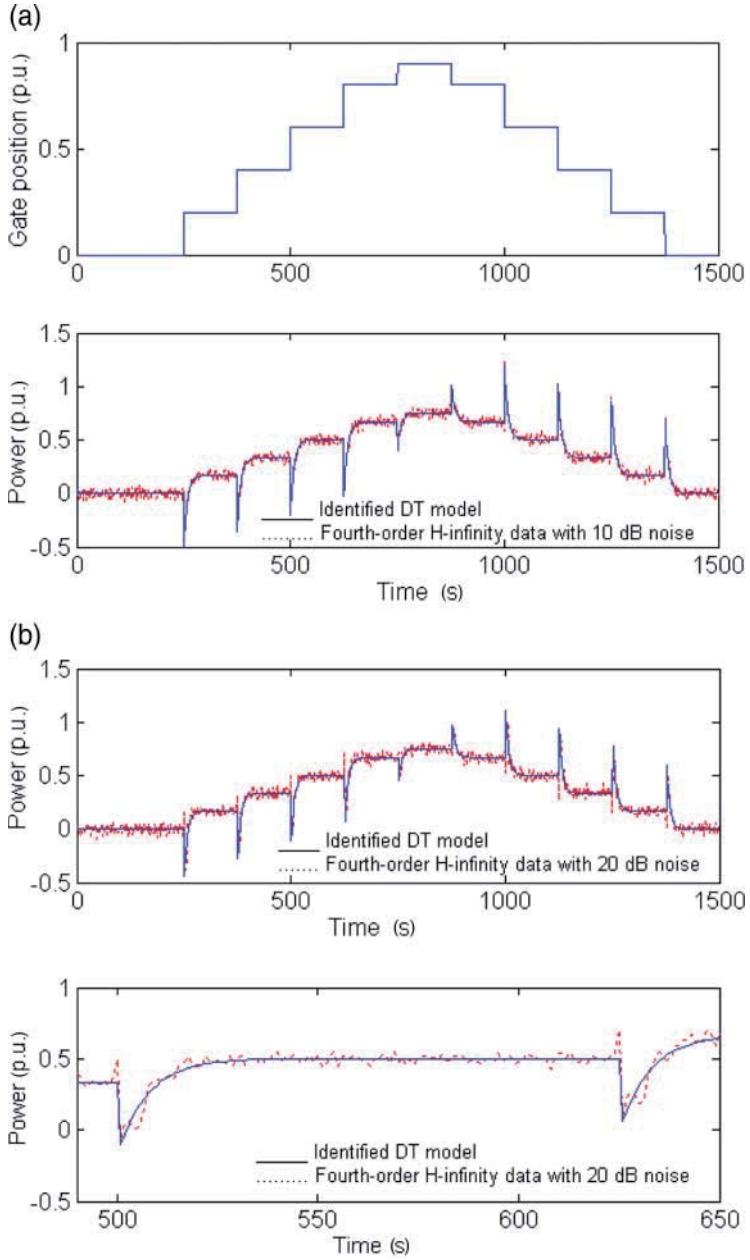

Figure 7. Output identification with multi-step input signal. (a) Simulated output with 10 dB SNR and identified output, (b) simulated output with 20 dB SNR and identified output and (c) zoomed: simulated output with 20 dB SNR and identified output.

5. Self-tuned regulation

The application of adaptive control theory to the governor design has found wide-spread research because of its role in eliminating some of the problems associated with the classical and modern control. These include self-tuning regulation, variable-structure control, etc. in the adaptation of the control law. Research work demonstrates the adaptive control to offer a solution over

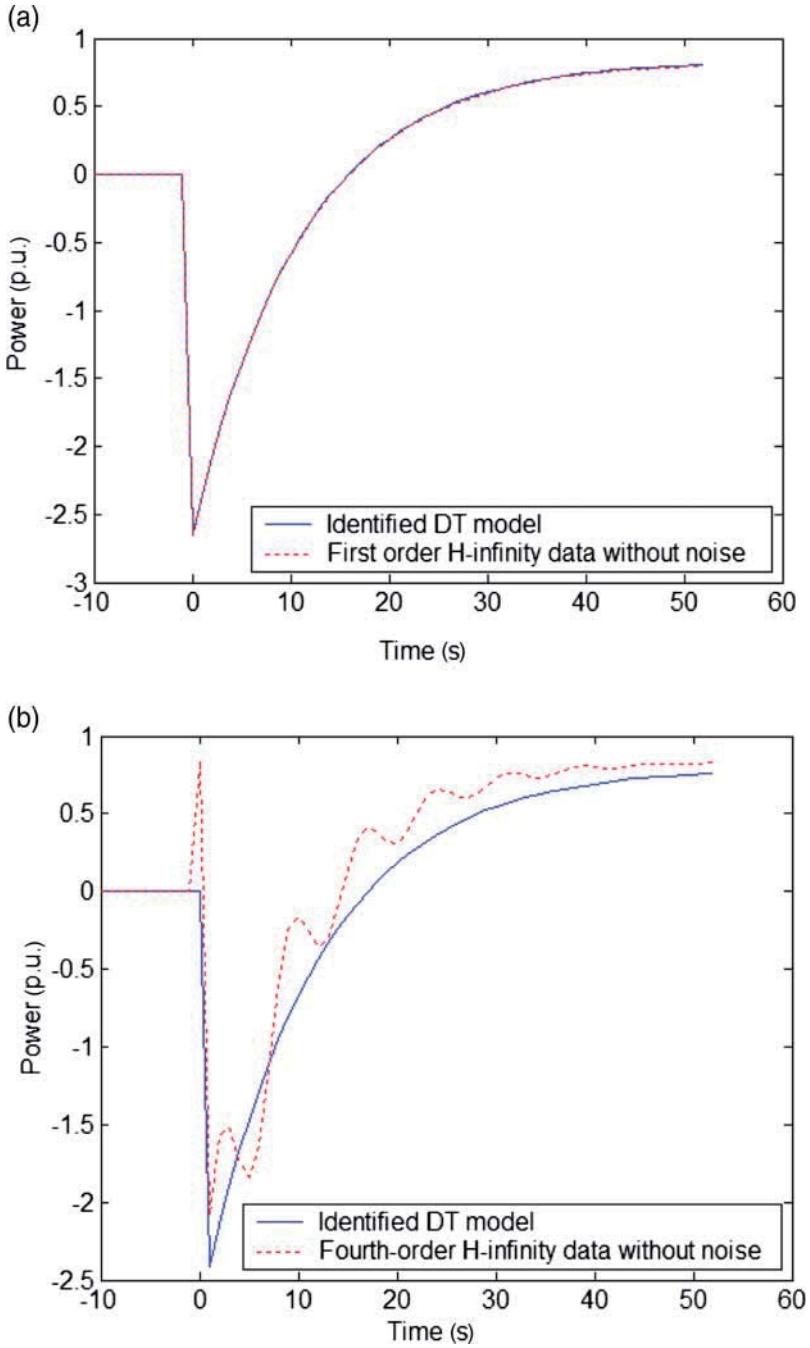

Figure 8. Identified output response to a unit step input test: (a) with FO H-infinity TF data without noise, (b) with FR H-infinity TF data without noise, (c) with FO H-infinity TF data with 20 dB SNR and (d) with FR H-infinity TF data with 20 SNR.

the drawbacks of classical techniques, through allowing the controller parameters to take into account the changes in the plant's operating conditions. The self-tuned regulation scheme as shown in Figure 12 consists of two loops; the inner loop between the parameter estimation and

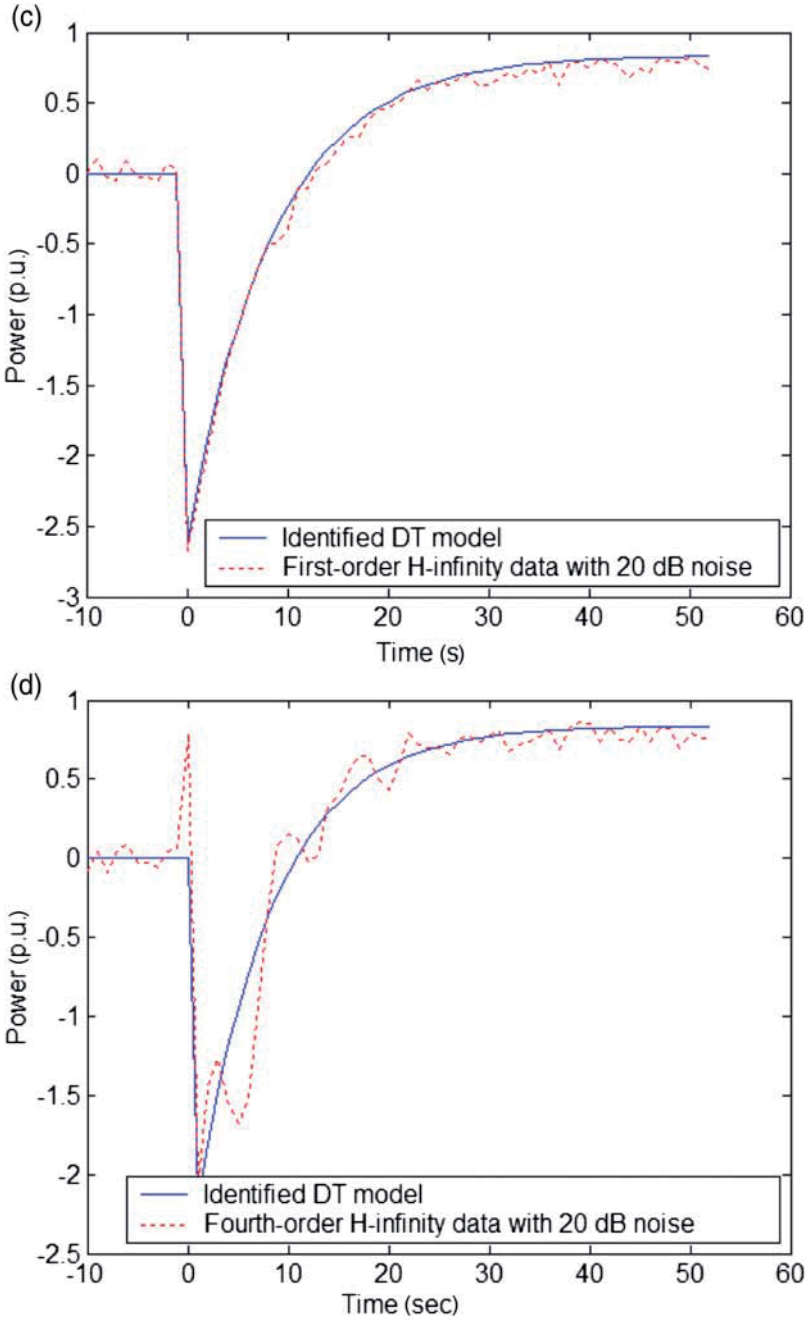

Figure 8. Continued.

the design computation, and the outer loop between plant and feedback regulators. To achieve adaptation, the most important aspect is the continuous estimation of plant model parameters. The identification of plant deals with the problem of developing mathematical models, based on observed data from the plant. There exist many techniques such as IVs, maximum likelihood, stochastic approximation and recursive least-square (RLS) algorithm, for the identification of the dynamical system.

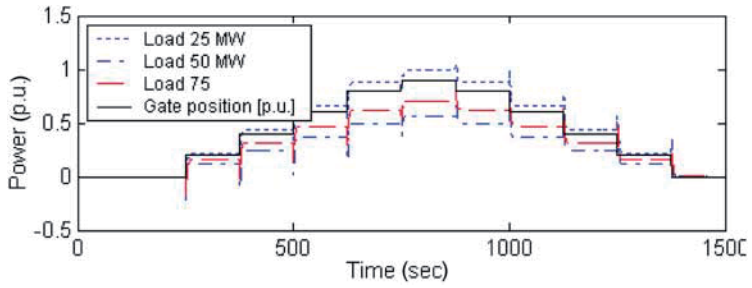

Figure 9. SYSFIT identified TF model simulation.

Once the estimated parameters of the identified model represent the true parameters of the plant, the next step that remains is the design of the self-tuned controller. A number of methods such as generalised minimum variance, pole-placement, PID control and LQ optimal can be found in the various literature (Swindenbank, Brown, and Flynn 1999). There are several PID controller structures and versions used in practice. The recurrent control algorithms which compute the actual value of the controller output $u_c(k)$ from the previous value $u_c(k-1)$ given as

$$u_c(k) = q_0 e(k) + q_1 e(k-1) + q_2 e(k-2) + u_c(k-1) \tag{16}$$

seems to be suitable.

$$\text{Where } q_0, q_1, q_2 = f(K_P, T_I, T_D, T_0). \tag{17}$$

The digital PID controller is obtained through the discretisation of the integral and derivative components of the above equation. A number of digital PID variants are derived; the forward rectangular, backward rectangular or trapezoidal methods used to discretise the integral component. Another version as in case of the backward rectangular method, the derivative component may be replaced by a four-point difference.

A number of problems associated with the application of self-tuned regulation to real problems include; (i) the need for persistent excitation to ensure that parameters of the model converge to their true values, (ii) the problems of bias in the parameter estimates, (iii) changes in model structure, (iv) disturbance or set-point changes (Gregorčič and Lightbody 2000). It is the last problem on which this paper has been focused for study. To derive the RLS estimation, rapidly track the changes in parameters, it is essential to utilise an exponential forgetting factor. When a highly nonlinear characteristic is driven by large set-point changes or disturbances, then there is rapid variation in the parameters of the model with similar dynamics to that of the system itself. There exist many variants of the RLS algorithm which exhibit different properties when used on-line for extended periods of time; RLS with the exponential forgetting factor and resetting the algorithm (EFRA) and the least-square mean with adaptive directional forgetting (LSMADF) (Bobál, Dostál, and Sysel 1999). EFRA places upper and lower bounds on the trace of the covariance matrix while maintaining a robustly valued forgetting factor. In the present study, HPP model is simulated with different available PID control variants as given in Table 4, wherein their corresponding number is given in the right column. The controller law is designed on the basis of the Zeigler–Nichols criterion for digital PID control configuration (Bobál, Dostál, and Sysel 1999).

The use of the self-tuned control approach to obtain closed-loop hydro-plant operation for the identification of speed/frequency deviation is already discussed in Kishor (2008). The author has explored this study with different variants of PID controller on the random load disturbance variation. The open-loop block diagram of the hydro-plant is illustrated in Figure 13

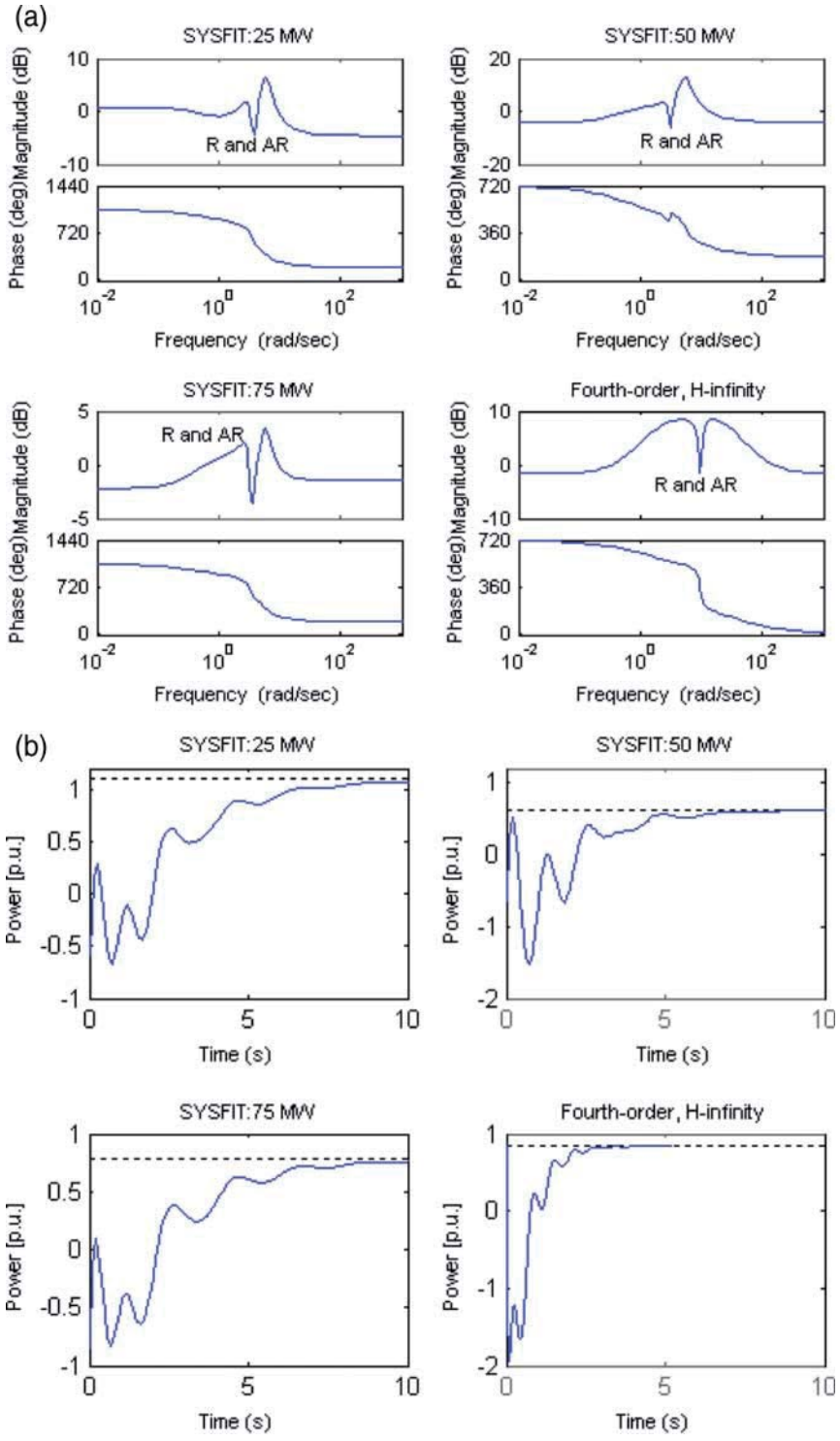

Figure 10. Comparison of TF models. (a) Frequency response and (b) time-domain response.

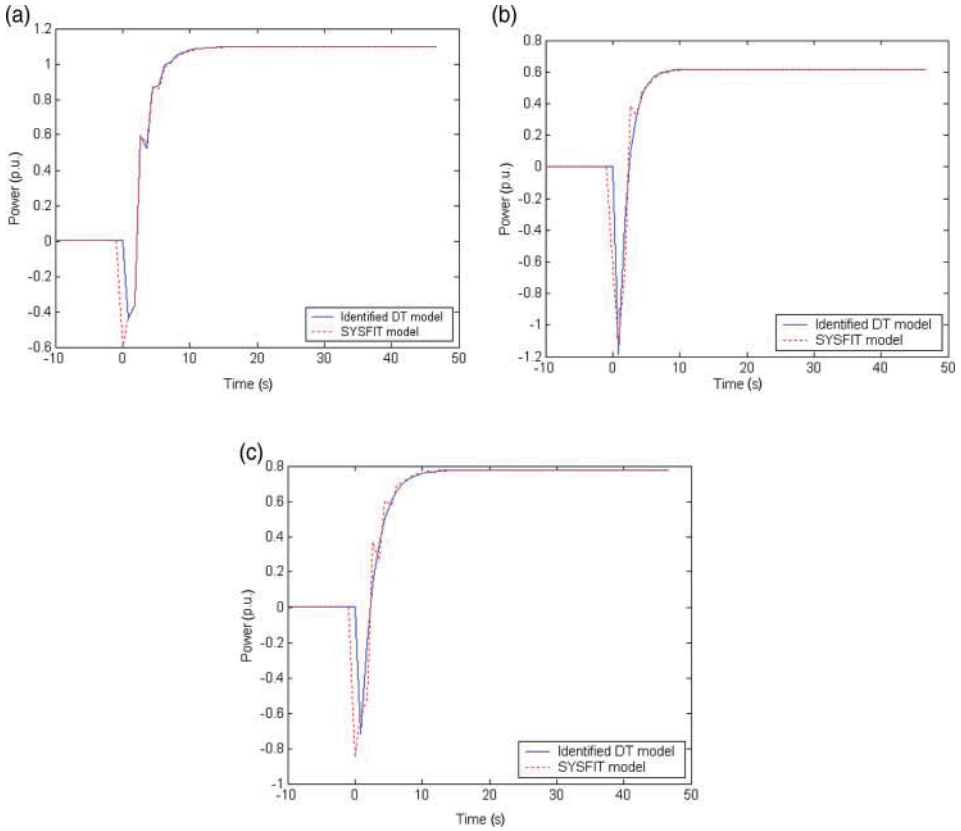

Figure 11. Output response of models to a unit step input test. (a) 25 MW load, (b) 50 MW load and (c) 75 MW load.

Table 3. Statistical attributes in modelling of SYSFIT TF.

Statistical measure	25 MW	50 MW	75 MW
YIC	0.999348	0.997616	0.997330
R_T^2	−13.89	−13.05	−12.01

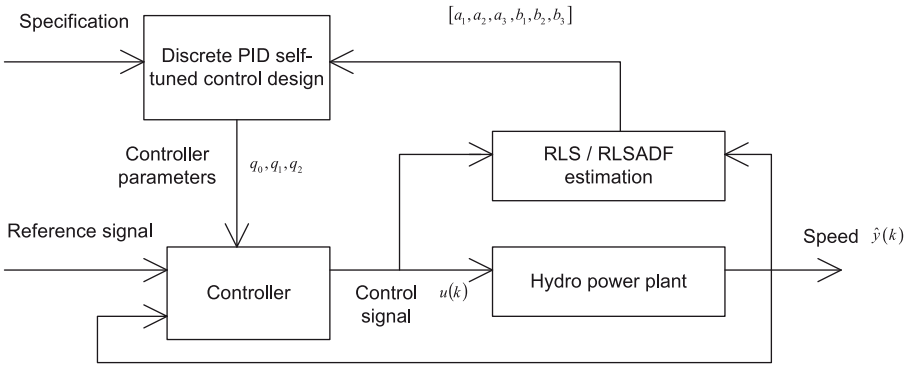

Figure 12. Self-tuning regulation approach as applied to HPP.

Table 4. PID controller design.

PID variants	No.
Forward rectangular method	C-1
Backward rectangular method	C-2
Trapezoidal rectangular method	C-3
Takahashi's	C-4
Forward rectangular, with replacement of derivation by a four point difference	C-5

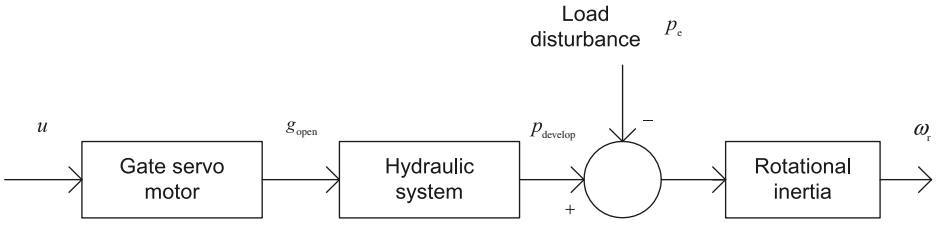

Figure 13. Block diagram of hydro plant in open-loop (without surge tank and tunnel effect).

comprising gate servomotor, hydraulic system (FO TF model), load disturbance and the turbine-generator set modelled as rotational inertia. The interested readers are advised to refer (Kishor 2008) for details on the methodology in the implementation of the said approach to the hydro-plant.

6. Discussion on simulation results of HPP with self-tuned approach

The control of turbine-generator unit dynamics in an isolated system is rather different than the synchronised one. Isolation of the plant may be either due to loss of synchronisation from the grid or off-grid operation in normal condition. The basic objective here is to restore the speed variation caused on disturbance, to its nominal value, in the shortest possible time.

This section presents the discussion on the results obtained in use of self-tuned technique to control turbine speed deviations in isolated operation during various conditions. The simulation study includes SO HPP TFs (both Padé and H-infinity), with different variants of DT controllers. The sensitivity studies are performed to determine the effect of varying plant parameters; WTC and MTC and different disturbances nature. The study includes step load increase, step reference change and simultaneous load and reference change disturbances.

6.1. *Step disturbance in load by 0.05 p.u. with constant speed reference*

In closed-loop operation of the plant, there exists a definite relationship between the speed response variation and its damping. As illustrated in Figure 14(a) and 14(b), it is observed that the value of MTC greatly determines the dip in speed deviation and its settling time. A value of 1 s shows a higher dip (up to 5%), smaller settling time and a value of 10 s that indicates lower dip, larger settling time; with progressive corresponding change as the MTC is changed from 1 to 10 s. Further, it is observed that a value of WTC as 4 s comparatively increases the dip in speed deviation (about 6%), for a given MTC, without affecting the settling time significantly. An off-set free response is attained. It is also seen that they all intersect at a specified point. The steady-state accuracy is strictly satisfied. A close observation in Figure 14(b) suggests that by the use of the adaptive directional forgetting factor; the weight of the current input–output data is determined

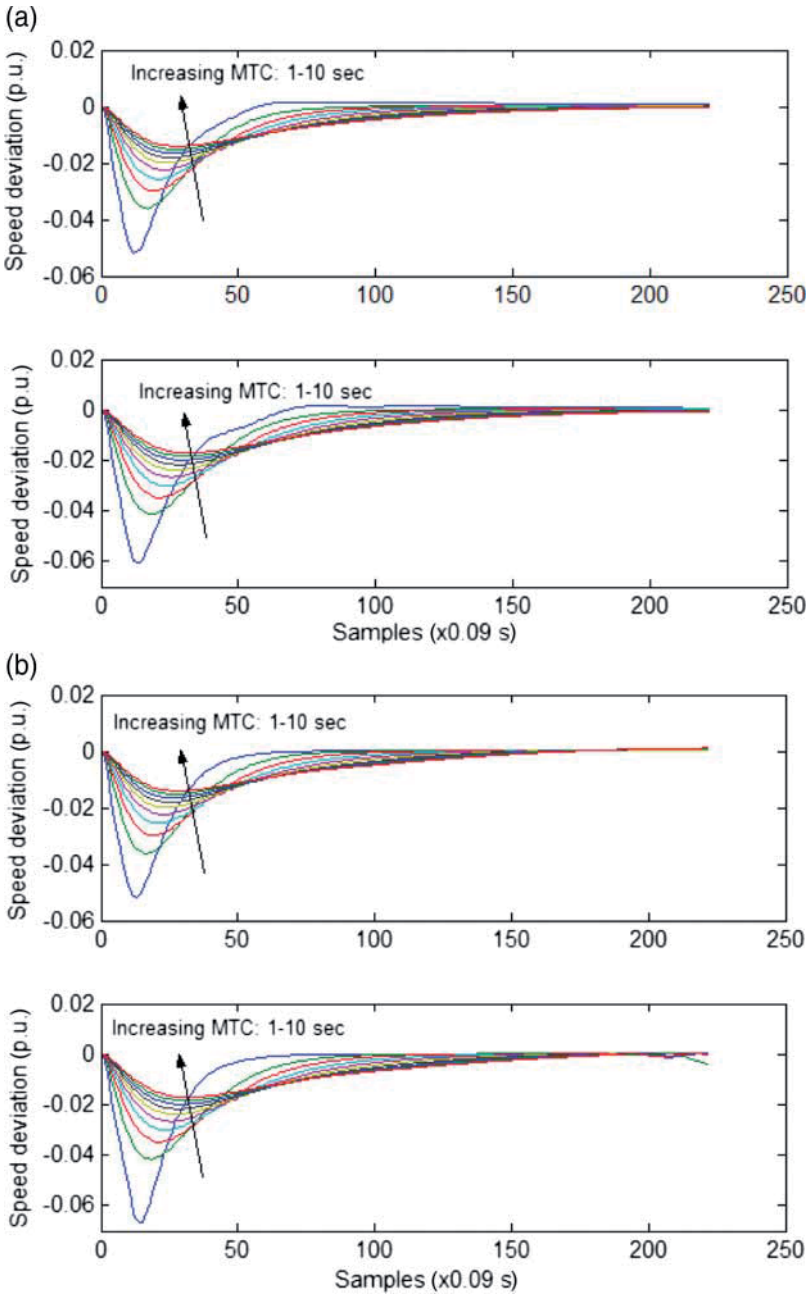

Figure 14. Simulated response of turbine-generator speed for step load disturbance by 0.05 p.u. with constant reference. Upper panel: WTC = 3 s; Lower panel: WTC = 4 s. (a) FO Padé TF with C-4 (LSM) and (b) FO Padé TF with C-4 (LSMADF).

with respect to input and output signal changes, thus resulting in a comparatively reduced settling time, without appreciable variation in the speed deviation dip. A quick correction action is offered by the controller. The graphical comparison of Figure 14 with a simulated response of H-infinity TF model indicates similar qualitative characteristics, and hence not shown in the paper.

6.2. *Step change in speed reference (0.02 p.u.) with constant load (0.01 p.u.)*

Next, it is desired to evaluate the performance of the controller when speed reference is changed with load applied on the plant. The analytical study is carried out for both Padé and H-infinity TFs along with different variants of controller; whereas, as an illustration, the performance with

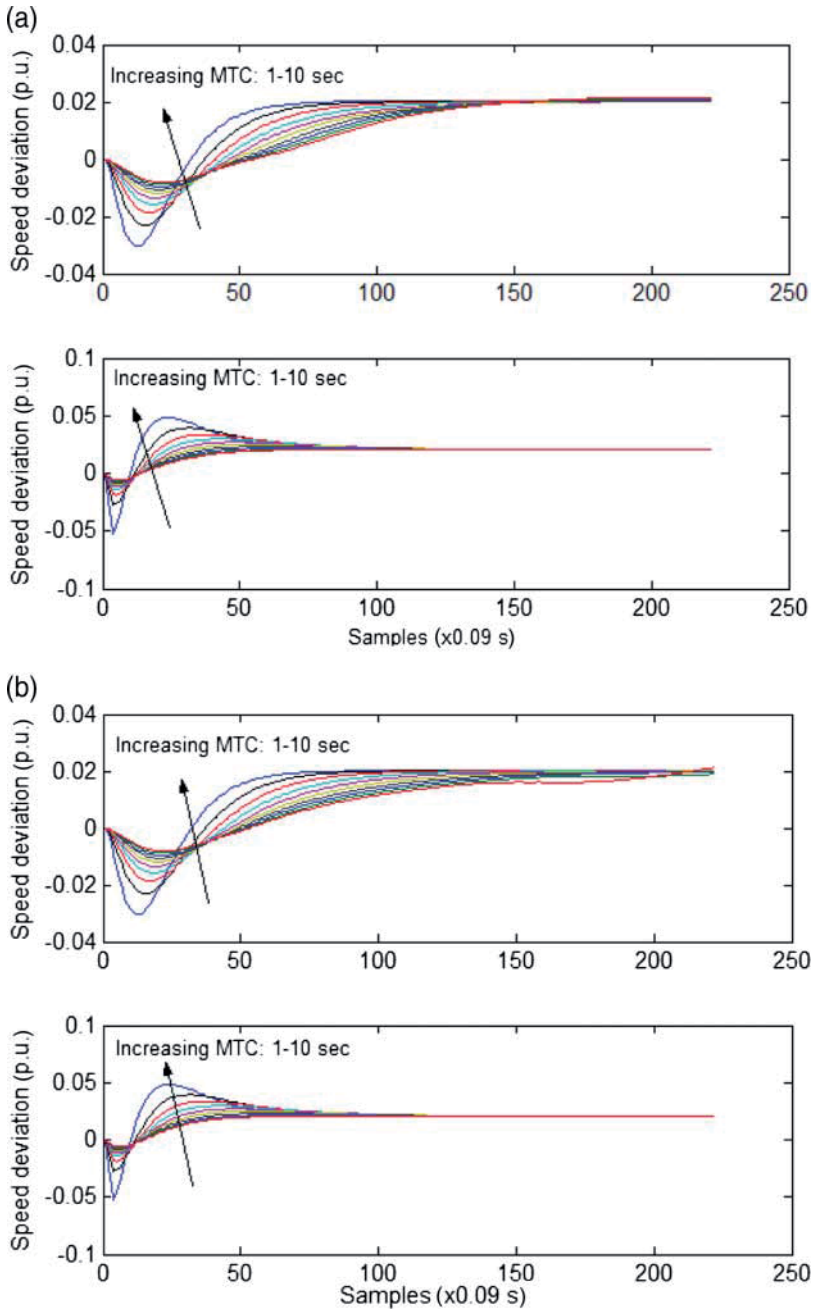

Figure 15. Simulated response of turbine-generator speed for step change in reference with a constant load. Upper panel: WTC = 3 s; Lower panel = 4 s. (a) FO H-infinity TF with C-3 (LSM), (b) FO H-infinity TF with C-3 (LSMADF), (c) FO Padé TF with C-3 (LSM) and (d) FO Padé TF with C-3 (LSMADF).

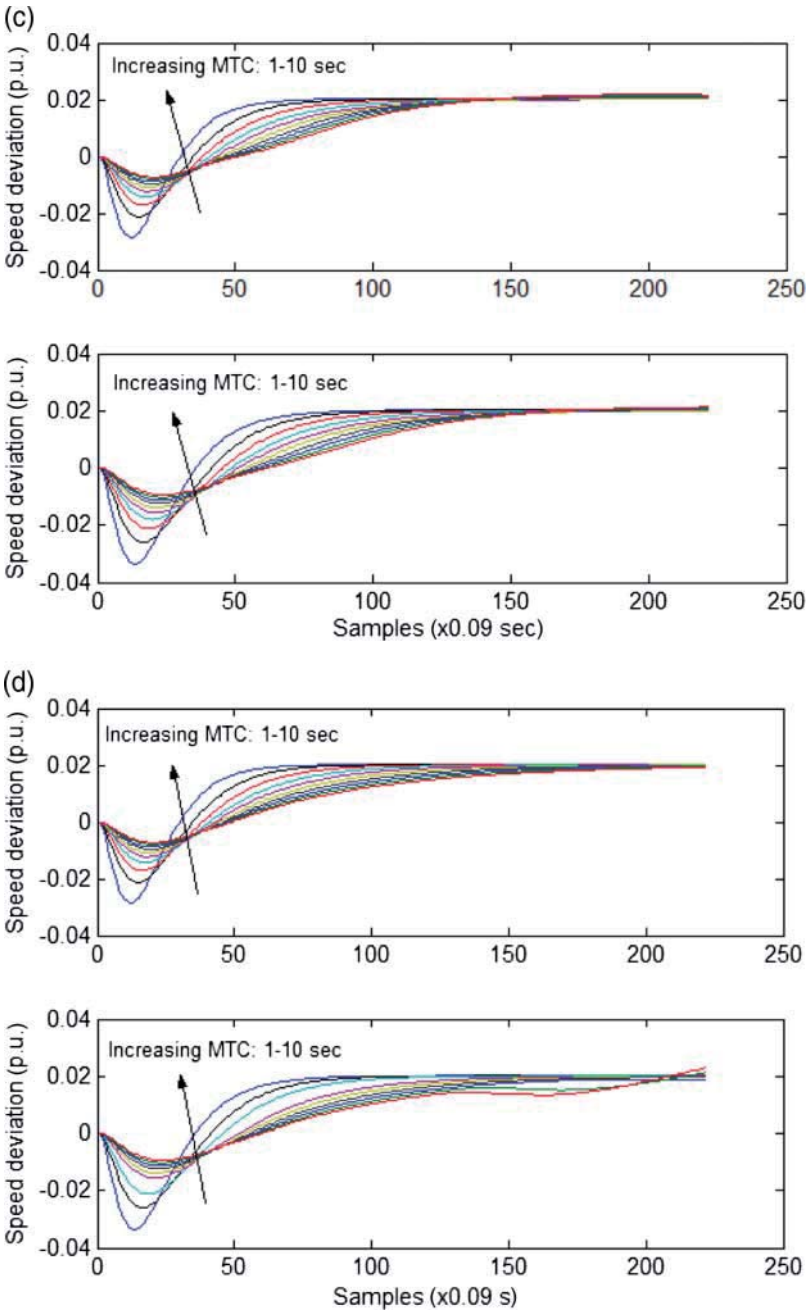

Figure 15. Continued.

controller C-3 only is given in the paper. The simulated results of Padé and H-infinity TFs for the above operating conditions are shown in Figure 15. It can be seen that although both TF models provide quite satisfactory performance; the response variation at the WTC as 3 s are identical (undershoot = 3%), however, H-infinity TF yields a smaller settling time at the expense of higher peak deviations (±5%) at a WTC equal to a value of 4 s. The responses due to both least-square mean (LSM) and LSMADF identification techniques are similar.

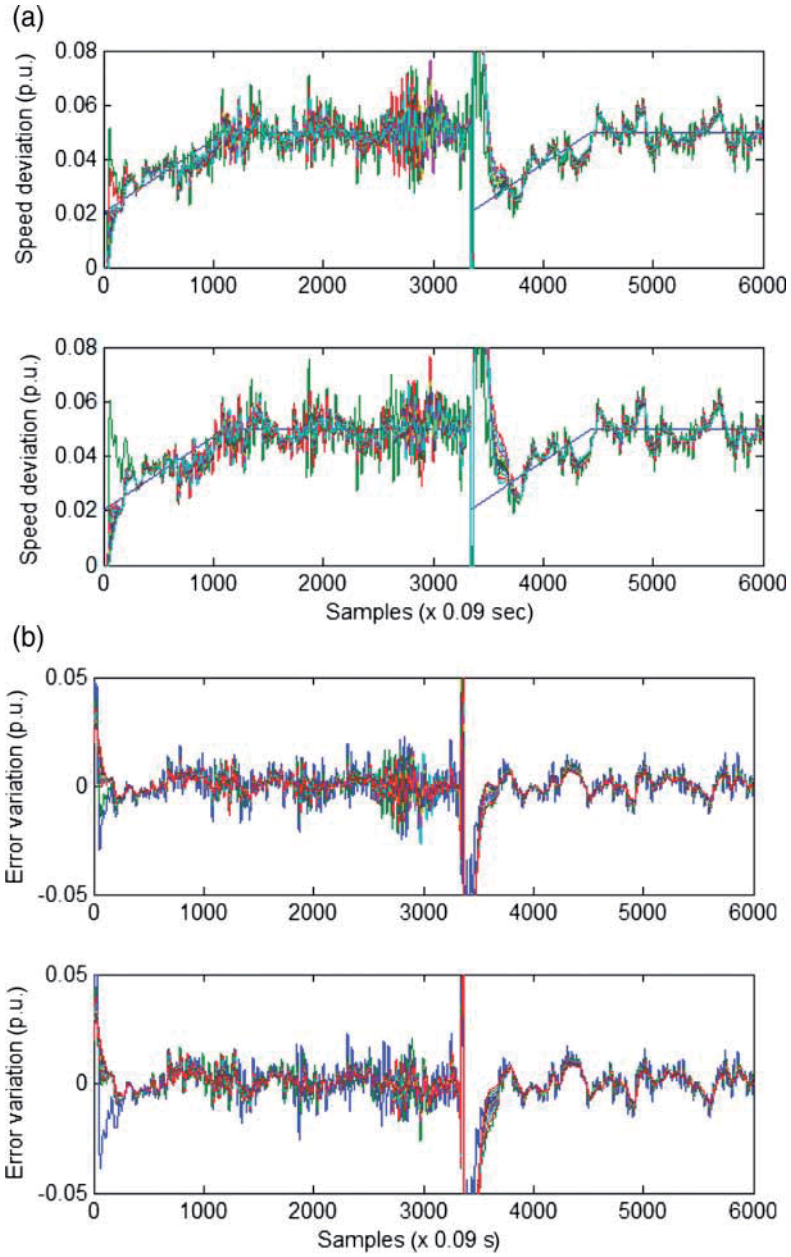

Figure 16. Simulated response of turbine-generator speed for simultaneous change in load disturbance and reference speed. Upper panel: WTC = 3 s; Lower panel: WTC = 4 s. (a) Reference track and (b) steady-state error.

6.3. *Simultaneous change in load disturbance and reference speed (0–0.05 p.u.)*

The study is carried out to demonstrate the dynamical behaviour of FO TF models along with controllers. The study involves an injection of a random signal as a load disturbance variation (0–0.05 p.u.). Due to space constraints, all the simulation results are not shown. Figure 16 depicts the performance of controller C-3 on FO Padé TF model. The MTC is changed from 1–10 s. The speed tries to track the given variation of the reference speed as observed in Figure 16(a) but

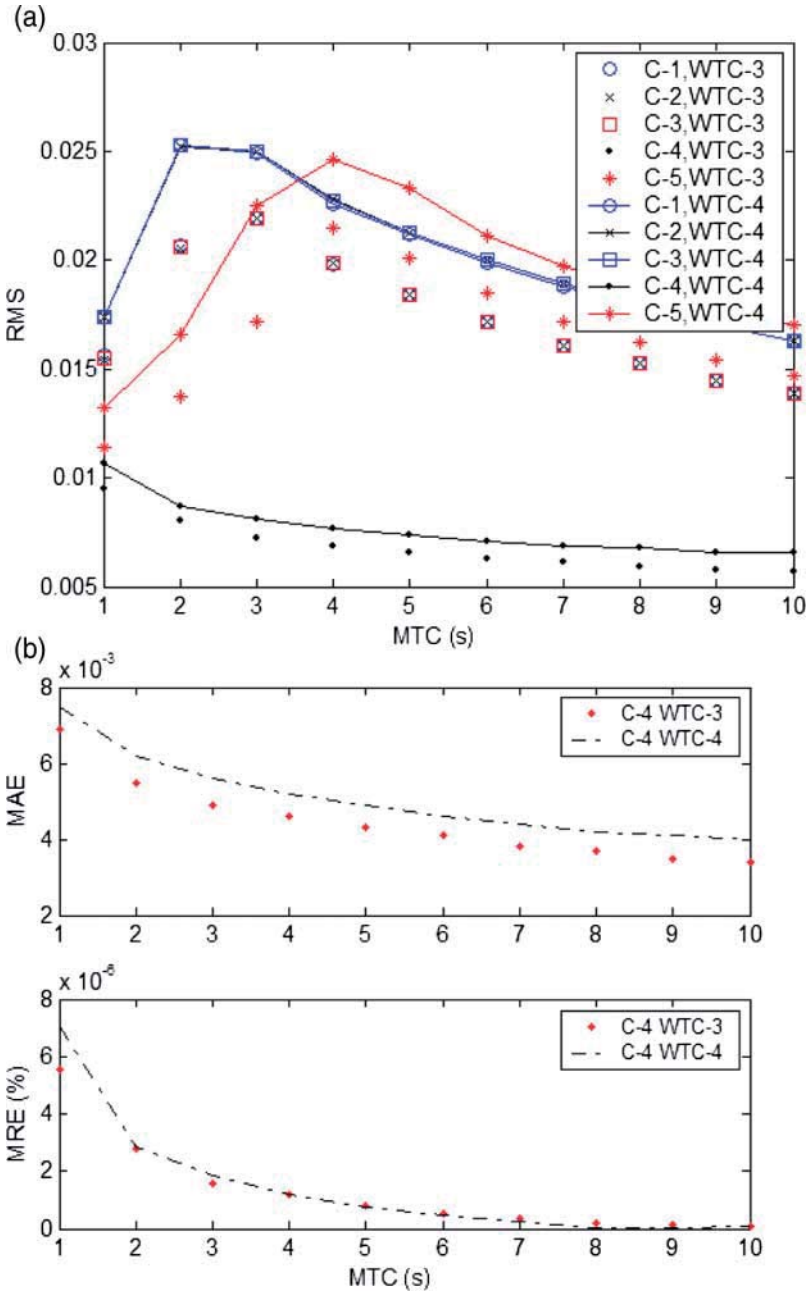

Figure 17. Performance assessment under PID control variant. (a) RMS tracking error and (b) MAE and MRE.

there is a delay between them. Though the steady-state error between turbine-generator speed and reference speed is small even with the inclusion of time-varying load disturbance, Figure 16(b) indicates that the control is stable, since the error remains along the zero scale. The speed deviation converges towards the analytical value as the specified period increases. A large steady-state error indicates a poor tracking of reference speed. As a measure of mismatch, the speed tracking error

over the period T_r is estimated in terms of root mean square, $\mathrm{RMS}_{\Delta w}$ given as

$$\mathrm{RMS}_{\Delta w} = \sqrt{\frac{1}{N_r}\sum_{i=1}^{N_r}(A_{ri} - \Delta w_i)^2}. \tag{18}$$

The other criterions used for measuring the performance are mean absolute error, $\mathrm{MAE}_{\Delta w}$ and mean relative error, $\mathrm{MRE}_{\Delta w}$ given as

$$\mathrm{MAE}_{\Delta w} = \frac{1}{N_r}\sum_{i=1}^{N_r}|A_{ri} - \Delta w_i|, \tag{19}$$

$$\mathrm{MRE}_{\Delta w}(\%) = \frac{1}{N_r}\sum_{i=1}^{N_r}\left|\frac{(A_{ri} - \Delta w_i)}{A_{ri}}100\right|, \tag{20}$$

where A_{ri} is the amplitude of the ramp signal, Δw_i is the frequency deviation and N_r is the signal samples.

From Equations (18) to (20), over the specified time period, the computed performance criterions are shown in Figure 17. The value suggests the tracking performance due to each of the PID variants. It reveals that the simulation with controller C-4 anticipates the random load disturbance and control action is relegated to a satisfactory corrective role, taking account of any difference between the turbine-generator speed and the reference speed with a minimum change on increasing MTC from 1–10 s.

The above discussion suggests that the response due to change in either (i) load, (ii) reference speed or (iii) both load and reference speed, the control action successfully attempts to minimise the speed deviation. The control strategy is extremely insensitive to changes in plant parameters and disturbances.

7. Conclusions

The work presented the dynamic simulation of the HPP to analyse the transient behaviour. The transient characteristics of approximated (up to FR) H-infinity and Padé TF models in response to different gate position changes were investigated. Time delay response in view of the WTC was analysed. The maximum rate of change in the turbine power is determined by the limit on opening/closing rate of gates. In the simulation of higher order models, a large magnitude change led to unwanted pressure-wave surges initially in turbine power response, nevertheless these transients could be limited with a small and constant rate of change in the gate position. The characteristic variations were greatly determined by parameter time-constants. The identified DT models could represent the FO dynamics successfully; without and with noise content in the output signal. However, the estimations for FR models were not accurately determined. The study needs to be further explored in this direction.

The identification algorithms were also verified on real hydro-turbine data on different load conditions in both frequency and time response.

The identify-then-control approach adapts the variation of the plant parameters and provides satisfactory response for every disturbance considered in study. Investigations revealed that the response of each controller differs marginally. The effect of wide range of changes in values of MTC and WTC on the speed deviation response remained typically low.

Nomenclature

symbols

D_{m}	damping coefficient
Δq	flow deviation (p.u.)
Δp	torque deviation (p.u.)
Δh	head deviation (p.u.)
$H(s)$	Laplace transform of Δh (p.u.)
$Q(s)$	Laplace transform of Δq (p.u.)
Z	Hydraulic surge impedance
T	time constant, s
q^{-1}	backward shift operator
B	output polynomial estimation parameter
A	input polynomial estimation parameter
WR^2	weight of all rotating parts multiplied by the square of the radius of gyration
p	number of parameters
F	hydraulic friction loss
Γ	area of penstock
L	length of penstock
K	controller gain

Greek symbols

ν	measurement noise
δ	me delay
σ	variance

Subscripts

m	mechanical
wp	water in penstock
t	turbine
develop	develop
open	open position
r	rotor
o	rated operating point
devia, p	deviation in penstock
p	penstock
e	elastic
y	discrete model output variable
u	discrete model input variable
k	sampling instant
i	iteration
c	controller
un	un-corrupted
P	proportional-gain
I, D	integral, derivative-gain time period

Al.-Amer, S. H., and F. M. Al.-Sunni. 2000. “Approximation of Delay Systems.” Proceedings of the American Control Conference, 2491–2495. Chicago, IL, June.

Bobál, V., P. Dostál, and M. Sysel. 1999. "Self-Tuning PID Controller using δ – Model Identification." The 7th Mediterranean Conference on Control and Automation (MED'99), Haifa, Israel, June 28–30, 1084–1098.
Captain Toolbox. Accessed December 10, 2007. http://www.es.lanes.ac.uk/cres/captain.
Eker, İ. 2004. "Governors for Hydro-Turbine Speed Control in Power Generation: A SIMO Robust Design Approach." *Energy Conversion and Management* 45: 2207–2221.
Fang, H., L. Chen, N. Dlakavu, and Z. Shen. 2008. "Basic Modeling and Simulation Tool for Analysis of Hydraulic Transients in Hydroelectric Power Plants." *IEEE Transactions on Energy Conversion* 23: 834–841.
Flores, J. J., and N. Pastor. 2005. "Time-Invariant Dynamic Systems Identification Based on the Qualitative Features of the Response." *Engineering Application of Artificial Intelligence* 18: 719–729.
Gregorčič, G., and G. Lightbody. 2000. "A Comparison of Multiple Model and Pole-Placement Self-Tuning for the Control of Highly Non-Linear Processes." Proceedings of the Irish Signals and Systems Conference, 303–311. Ireland, June.
Hagihara, S., H. Yokota, K. Gode, and K. Isobe. 1979. "Stability of a Hydraulic Turbine Generating Unit Controlled by PID Governor." *IEEE Transactions on Power Apparatus and Systems* PAS-98: 2294–2298.
Kishor, N. 2008. "Zero-Order TS Fuzzy Model to Predict Hydro Turbine Speed in Closed Loop Operation." *Applied Soft Computing* 8: 1074–1084.
Kishor, N., S. P. Singh, and A. S. Raghuvanshi. 2006. "Dynamic Simulation of Hydro Turbine and its State Estimation Based LQ Control." *Energy Conversion and Management* 47: 3119–3137.
Lansberry, J. E., L. Wozniak, and D. E. Goldberg. 1992. "Optimal Hydrogenerator Governor Tuning with a Genetic Algorithm." *IEEE Transactions on Energy Conversion* 7: 623–630.
Lam, J. 1993. "Model Reduction of Delay Systems using Padé Approximations." *International Journal of Control* 57: 377–391.
Mansoor, S. P., D. I. Jones, D. A. Bradley, F. C. Aris, and G. R. Jones. 2000 "Reproducing Oscillatory Behaviour of a Hydroelectric Power Station by Computer Simulation." *Control Engineering Practice* 8: 1261–1272.
Murthy, M. S. R., and M. V. Hariharan. 1983. "Analysis and Improvement of the Stability of a Hydro-Turbine Generating Unit with Long Penstock." *IEEE Transactions on Power Apparatus and Systems* PAS-102: 360–367.
Nicolet, C., B. Kawkabani, B. Greiveldinger, J.-J. Herou, P. Allenbach, and J.-J. Simond. 2007. "Turbine Speed Governor Parameters Validation in Islanded Production." 2nd IAHR International Meeting of the Workgroup on Cavitation and Dynamic Problems in Hydraulic Machinery and Systems. Timisoara, October 24–26.
Sanathanan, C. K. 1987. "Accurate Low Order Model for Hydraulic Turbine-Penstock." *IEEE Transactions on Energy Conversion* EC-2: 196–200.
Söderström, T., and P. Stoica.1989. *System Identification*. Hemel Hempstead, UK: Prentice-Hall.
Swindenbank, E., M. D. Brown, and D. Flynn. 1999. "Self-Tuning Turbine Generator Control for Power Plant." *Mechatronics* 9: 513–537.
Trudnowski, D. J. 1992. *Frequency Domain Transfer Function Identification using the Computer Program SYSFIT, PNL-8455*. Richland, WA: Pacific Northwest Laboratory.
Trudnowski, D. J., and J. C. Agee. 1995. "Identifying a Hydraulic-Turbine Model from Measured Field Data." *IEEE Transactions on Energy Conversion* 10: 768–773.
Young, P. C. 1984. *Recursive Estimation and Time-Series Analysis*. Berlin: Springer-Verlag.
Zeng, Y., L. Zhang, T. Xu, and H. Dong. 2011. "Building and Analysis of Hydro Turbine Dynamic Model with Elastic Water Column." Asia-Pacific Power and Energy Engineering Conference, China, Wuhan, March 24–28.

Appendix

$$a_{11} = 0.3 \text{ p.u.}; \quad a_{12} = 0.82 \text{ p.u.}; \quad a_{13} = 0.387 \text{ p.u.}; \quad a_{21} = 1.276 \text{ p.u.}; \quad a_{22} = 0.839 \text{ p.u.};$$
$$a_{23} = -0.553 \text{ p.u.}; \quad T_{\text{wp}} = 3, 4, 5\&6\ s; \quad T_{\text{m}} = 1 - 10\ s; \quad T_{\text{gv}} = 0.5 \text{ p.u.}; \quad D_{\text{m}} = 2.0$$